N-Glycans on the extracellular domain of the Notch1 receptor control Jagged-1 induced Notch signalling and myogenic differentiation of S100β resident vascular stem cells

Eoin Corcoran[1], Abidemi Olayinka[1], Mariana di Luca[1], Yusof Gusti[1],
Roya Hakimjavadi[1], Brendan O'Connor[2], Eileen M. Redmond[3] and Paul A. Cahill[1]*

[1] Vascular Biology and Therapeutics Laboratory, School of Biotechnology Faculty of Science and Health, Dublin City University, Dublin, Ireland.

[2] School of Biotechnology Faculty of Science and Health, Dublin City University, Dublin, Ireland

[3] Department of Surgery, University of Rochester, 601 Elmwood Ave, Rochester, NY 14642, United States

Abstract

Notch signalling, critical for development and postnatal homeostasis of the vascular system, is highly regulated by several mechanisms including glycosylation. While the importance of O-linked glycosylation is widely accepted, the structure and function of N-glycans has yet to be defined. Here, we take advantage of lectin binding assays in combination with pharmacological, molecular, and site-directed mutagenetic approaches to study N-glycosylation of the Notch1 receptor. We find that several key oligosaccharides containing bisecting or core fucosylated structures decorate the receptor, control expression and receptor trafficking, and dictate Jagged-1 activation of Notch target genes and myogenic differentiation of multipotent S100β vascular stem cells. N-glycans at asparagine (N) 1241 and 1587 protect the receptor from accelerated degradation, while the oligosaccharide at N888 directly affects signal transduction. Conversely, N-linked glycans at N959, N1179, N1489 do not impact canonical signalling but inhibit differentiation. Our work highlights a novel functional role for N-glycans in controlling Notch1 signalling and differentiation of vascular stem cells.

Teaser

A sweet development in Notch regulation of vascular smooth muscle cell differentiation

Introduction

Notch signalling is crucial for the development and postnatal homeostasis of the vascular system [1]. It has been implicated in cardiovascular disease, cancer, and neurological and

kidney disease. The Notch pathway is activated by interaction of receptors (Notch1–4) and ligands (Delta-like 1, 3, 4, and Jagged 1, 2) present on the surface of adjacent cells [3]. This interaction triggers sequential cleavage events resulting in release of the active form of Notch i.e., Notch intracellular domain (NICD). NICD translocates into the nucleus and, in combination with the transcription factor recombinant binding protein for the immunoglobulin region kJ (RBPJ, also known as CBF1/Suppressor of Hairless/LAG1, CSL) and the Mastermind-like (MAML 1–3) adaptor proteins, activates target genes including HES (Hairy and Enhancer of Split) and HEY (Hairy/enhancer-of-split related) that are essential modulators of neuronal, endocrine, and cardiovascular cell fate [4]. The Notch pathway may also be activated in the absence of 'canonical' ligands and independent of γ-secretase proteolytic cleavage; this non-canonical Notch signalling modulates Wnt/β-catenin, mammalian target of the rapamycin 2 complex (mTORC2)/Akt, Nuclear Factor kappa B (NF-κB), IkB kinase (IKK)-α/β and phosphatase and tensin homolog (PTEN)-induced kinase (PINK1) [5].

Notch impacts arterial pathology including atherosclerotic plaque development [6–10]. There is compelling evidence for the involvement of (i) differentiated medial vascular smooth muscle cells (SMC) that are stem cell antigen-1 positive (Sca1+) [11-12] and (ii) various adventitial [13-14] and medial progenitors [15–18] [19-20] in progressing vascular lesion formation through the accumulation of 'SMC-like' cells. Notch signalling decreases SMC differentiation marker expression [21] and promotes SMC-like cell accumulation within lesions [10]. Multiple studies describe the ability of Notch signalling to induce myogenic differentiation of stem cell populations such as C3H 10T1/2 embryonic fibroblasts, mesenchymal stromal stem cells and neural crest stem cells [22–24]. While the exact mechanism and cell(s) involved by which Notch and its target genes affect lesion formation remains incompletely understood, there is substantial evidence suggesting that the Notch1 receptor in particular [8, 10], plays a pivotal role in this process.

The Notch signalling pathway is tightly regulated by several mechanisms including cis-inhibition, negative feedback loops and PEST ubiquitination [25, 26] and by glycosylation of the Notch receptor [27]. There are several highly conserved glycosylation sites along the extracellular domain of the Notch receptor, most of which harbour O-linked glycans. Conserved sites of O-glycosylation on Notch were first discovered at the turn of the century in Drosophila melanogaster [28] and this gave rise to a wave of research centred on O-glycosylation of Notch, resulting in many more consensus sites and several important glycosyltransferases, such as Fringe, being identified [29, 30]. In contrast, very little is known about the specifics of N-linked glycosylation of Notch. It has been established that there are six N-glycosylation consensus sites along the extracellular domain of Notch [31] and that N-glycans are certainly present on the Notch receptor [34] but the number of these sites that are glycosylated, the structures of these N-glycans and their potential role in Notch signalling, remains unknown.

The impact of N-glycan decoration of key proteins on a given process can be revealed using chemical inhibitors of N-glycosylation. Tunicamycin (TNC), an antagonist for the GlcNAc phosphotransferase (GPT) enzyme, catalyses a critical step in the protein N-glycosylation pathway, linking the growing polypeptide to a dolichol precursor [32]. 1-deoxymannojirimycin (DMJ) blocks the trimming of the 14-sugar dolichol precursor oligosaccharide by inhibiting the mannosidase I enzyme and preventing the synthesis of complex or hybrid-type N-glycans [33]. Because the specificities of these inhibitors are broad, a more targeted approach for regulating N-glycans can be achieved using siRNA

knockdown of key glycosyltransferases, Fut8 and Mgat3. A family of glycosyltransferases known as N-acetylglucosaminyl transferases (GnT's) are responsible for the addition of GlcNAc residues to N-linked glycans. There are six members of this family (GnT-I to GnT-VI), all of which operate in the Golgi apparatus [34]. GnT-III (coded by the Mgat3 gene) catalyses the addition of a GlcNAc residue through a β-1,4 linkage to the β-mannose in the tri-mannosyl core of a growing N-linked oligosaccharide, creating a structure known as a bisecting N-glycan [35]. This structure has been shown to inhibit the addition of sugar residues by other glycosyltransferases such as GnT-II, GnT-IV and Fut8 [36, 37]. Bisecting N-glycans are heavily involved in the regulation of several cellular processes, including cell adhesion, protein degradation and growth factor signalling [38]. Members of the fucosyltransferase (FUT) family of enzymes facilitate the addition of fucose residues to the core N-glycan structure [39] in a process known as core fucosylation. Fut8 catalyses the transfer of fucose from a donor substrate to the asparagine-149 bound GlcNAc at the base of an N-glycan via an α1,6-linkage [40]. Core-fucosylated N-glycans regulate a wide array of cellular processes such as the expression of essential cadherins and the function of specific types of immunoglobulins [41-42]. As of yet, it has not been established whether N-glycans on the Notch1 receptor are core fucosylated, though it has been noted that aberrant activity of both Fut8 and Notch is regularly observed in cancer [43].

Of note, lectins have become powerful tools to determine the N-glycan profile of a glycoprotein, as they are highly specific carbohydrate-binding proteins with no catalytic activity [44]. They can bind mono- or oligosaccharides and can recognise and distinguish between distinct branching and linkage patterns [45]. Several assays have been developed and optimised which exploit the high level of specificity seen in lectin-oligosaccharide binding to determine the glycosylation profile of a given glycoprotein sample. The enzyme-linked lectin assay (ELLA) is a simple and rapid method of glycan analysis that, unlike techniques such as mass spectrometry and HPLC, does not require the chemical or enzymatic removal of carbohydrates from proteins [46]. In this way, lectins can be used to detect changes in N-glycosylation patterns following inhibitory interventions.

The aim of this study was to characterise the profile of N-glycosylation of the Notch1 receptor and explore the impact of these N-glycans on Notch signalling, receptor trafficking and Notch-mediated myogenic differentiation of stem cells *in vitro*.

Results

Jagged-1 (Jag-1) activation of the Notch1 receptor promotes myogenic differentiation

The phenotype of mouse aortic vascular stem cells (mVSCs) and C3H10T1/2 embryonic fibroblasts were assessed by immunocytochemistry. Cultured mouse smooth muscle cells (SMCs) (MOVAS-SMCs) served as a positive control for myogenic SMC differentiation marker expression. The mVSCs and C3H 10T1/2 cells were both positive for S100β and Sca1 expression, while negative for SMC markers, Cnn1 and Myh11 [Suppl Figure 1(a), Figure 1(a)]. The stemness of isolated S100β mVSCs was confirmed by demonstrating increased telomere length and telomerase activity when compared to aortic tissue and cultured SMCs [Suppl Figure 1(b), (c)]. Adipogenic (*Lpl* and *Fabp4*) and osteogenic gene expression (*Alpl* and *Sost*) was significantly increased following treatment of S100β mVSCs with lineage specific differentiation media, when compared to the maintenance media control [Suppl Figure 1(d), (e)]. These data confirm the phenotype and stemness of

138 the S100β mVSCs as distinct from freshly isolated aortic SMCs and aortic SMCs in
139 culture.

140 Immobilised recombinant Notch ligand, Jagged-1 increased the number of SMC-
141 like/myogenic Cnn1 positive cells (40.5 ± 5%, $p<0.05$ n=6) in S100β mVSCs cultures,
142 when compared to the Fc-IgG control (0.1 ± 0.4%) [Figure 1(b), (c)] concomitant with a
143 significant increase in the expression of Notch target gene, *Hey1* and the SMC
144 differentiation marker gene, *Myh11*, an effect attenuated following pre-treatment of the
145 cells with the γ-secretase inhibitor, DAPT [Figure 1(d),(e)]. As the Notch1 receptor has
146 been implicated in arteriosclerotic lesion formation [8, 10, 49], the effect of Notch1
147 receptor depletion following siRNA knockdown on Jagged-1 induced *Hey1* and *Myh11*
148 expression was also assessed in S100β mVSCs [Figure 1(g), (h)]. The transfection
149 efficiency of the siRNA's was confirmed at > 80% under optimised conditions using a
150 fluorescently- tagged siRNA (TYE 563 DsiRNA) [Suppl Figure 2(a)]. *Notch1* mRNA
151 levels [Suppl Figure 2(b)] and Notch1 receptor protein levels [Suppl Figure 2(c)] were
152 significantly reduced when compared to the scrambled control concomitant with a
153 significant inhibition of Jagged-1 induced *Hey1* [Figure 1(d)] and *Myh11* [Figure 1(e)]
154 expression.

155 These data confirm that multipotent S100β mVSCs and C3H10T1/2 cells respond to
156 Notch ligand-induced activation of Notch signalling to promote myogenic differentiation
157 of these cells via activation of the Notch1 receptor.

158 **Chemical inhibition of N-glycosylation impairs Jagged-1 induced Notch signalling**

159 N-glycan analysis was first assessed in whole cell lysates before immunoprecipitated
160 Notch1 was prepared, and lectin binding evaluated using a series of commercial lectins
161 (Table I). Ectopic overexpression of a plasmid-encoded Notch1 was achieved using cells
162 transfected with either *pCS2 Notch1 Full Length-6MT* or *pCS2 Notch1 ICv-6MT* plasmids
163 [Suppl Figure 3(a)]. Samples were immuno-probed using an anti-myc-tag antibody and
164 stained for either the myc-tagged Notch1 or myc-tagged NICD, or an anti-β-actin
165 antibody, which served as the loading control [Suppl Figure 3(b)].

166 TNC and DMJ are both chemical inhibitors of N-glycosylation [32-33]. Cells were treated
167 with different concentrations of TNC (0.3 - 0.7μg/mL) or DMJ (2.0 - 4.0μg/mL) before
168 lectin binding was assessed in whole cell lysates using the ELLA assay. The binding
169 characteristics of each lectin have previously been described (Table I, [46]). There was a
170 dose-dependent decrease in absorbance, indicating a reduction in lectin binding, following
171 treatment of S100β mVSCs with TNC when compared to the non-treated control [Figure
172 2(a)]. Maximum inhibition was observed at 0.5μg/mL (in the cases of WGA and E-PHA).
173 Similarly, DMJ treatment caused a significant reduction in binding across all lectins
174 compared to the non-treated control with maximal inhibition observed at 4.0μg/mL
175 [Figure 2(c)]. A similar dose-dependent decrease in lectin binding was observed in whole
176 lysates following treatment of C3H10T1/2 cells with TNC [Suppl Figure 4(a)] and DMJ
177 [Suppl Figure 4(b)], but only in WGA and E-PHA. No significant change in binding was
178 detected at any DMJ concentration with ConA or LCA [Suppl Figure 4(b)]. These data
179 confirm the optimal concentrations of TNC and DMJ required to reduce lectin binding in
180 whole cell lysates. After establishing the effect of TNC and DMJ in whole cell lysates,
181 their effect on the N-glycan profile of the immunoprecipitated Notch1 receptor was
182 assessed.

183 Immunoprecipitated Notch1 was prepared following optimisation of the
184 immunoprecipitation protocol from whole cell lysates [Suppl Figure 2(d)]. Lectin binding
185 was significantly reduced in the immunoprecipitated Notch1 preparation from S100β
186 mVSCs treated with both TNC [Figure 2(b)] and DMJ [Figure 2(d)] across all lectins
187 other than WGA. Inhibition by DMJ was as pronounced as that of TNC. The
188 repercussions of removing these N-glycans from the Notch1 receptor on Jagged 1-induced
189 Notch signalling and myogenic differentiation of S100β mVSCs and C3H10T1/2 cells
190 was assessed. Increased *Hey1* and *Myh11* expression following treatment with
191 recombinant Jagged-1, when compared to the control IgG-Fc, was significantly reduced in
192 TNC [Figure 2(e),(f)] and DMJ [Figure 2(g),(h)] treated S100β mVSCs. In a similar
193 manner, recombinant Jagged-1 significantly increased *Hey1* and *Myh11* expression in
194 C3H10T1/2 cells when compared to IgG-Fc, an effect that was significantly reduced in
195 TNC treated [Suppl Figure 4(d), (e)] and DMJ treated cells [Suppl Figure 4(f), (g)].
196 Interestingly, TNC treatment also led to a significant decrease in *Hey1* expression in the
197 Fc-treated control sample [Suppl Figure 4(d)]. The decrease in *Hey1* expression following
198 treatment of S100β mVSCs with TNC and DMJ was not due to changes in the expression
199 of the Notch1 receptor as there was no significant change in either *Notch1* transcript levels
200 or Notch1 protein expression following TNC or DMJ treatment, compared to the non-
201 treated control [Suppl Figure 3(c), (d)].

202 Notch intracellular domain (NICD) can activate Notch signalling independent of ligand
203 binding; this function was exploited to determine whether TNC and DMJ affected key
204 Notch signalling downstream of receptor activation. Ectopic expression of the Notch1
205 NICD [Suppl Figure 3(a), (b)] significantly increased the expression of the Notch target
206 gene *Hey1* in S100β mVSCs [Figure 3(a), (c)]. There was no significant change in this
207 response following TNC or DMJ treatment of these cells [Figure 3(a), (c)]. Similarly,
208 expression of the myogenic marker *Myh11* was increased following ectopic expression of
209 NICD [Figure 3(b), (d)]. However, this response was significantly attenuated by treatment
210 with either TNC or DMJ [Figure 3(b), (d)). These data suggest that Notch pathway
211 elements between the cleavage of the NICD and the activation of *Hey1* gene are
212 unaffected by TNC or DMJ, but components of the myogenic differentiation pathway are
213 altered by these treatments.

214 Collectively, these data show that inhibition of global glycosyltransferase activity with
215 TNC and DMJ reduced the level of N-glycan structures on cellular glycoproteins within
216 whole lysates from S100β mVSCs and C3H10T1/2 cells. This includes Notch1 as both
217 inhibitors had a significant effect on the N- glycosylation profile of the purified
218 immunoprecipitated receptor, supporting the presence of N-glycans on Notch1. Removal
219 of these N-glycans caused a significant reduction in ligand-induced Notch signalling and
220 myogenic differentiation in these cells. As downstream components of Notch signalling
221 and myogenic differentiation pathways following ectopic expression of Notch1 NICD
222 were not altered by *TBC* or *DMJ*, their effect appears to be primarily at the level of the
223 Notch1 receptor.

224 **GnT-III and Fut8 depletion impairs Jagged-1 induced Notch signalling**

225 *Mgat3* and *Fut8* genes code for the glycosyltransferases GnT-III and Fut8, respectively.
226 To deplete their levels, targeted siRNA knockdown was performed in S100β mVSCs
227 [Suppl Figure 3(e), (f)] and C3H10T1/2 cells [Suppl Figure 5(a), (b)], respectively, before
228 the N-glycan profile of whole lysates [Figure 4(a)] and immunoprecipitated Notch1

229 [Figure 4(b)] was assessed by lectin binding using the ELLA assay. There was a
230 significant reduction in lectin binding of whole lysates following *Mgat3* knockdown for
231 ConA and E-PHA lectins in both S100β mVSCs [Figure 4(a)] and C3H10T1/2 cells
232 [Suppl Figure 4(c)] compared to the scrambled control, while no significant reduction in
233 binding was detected with the LCA or WGA lectins. In the case of the *Fut8* knockdown,
234 this led to a significant decrease in LCA binding in both cell lines, while any changes in
235 binding with the other three lectins was statistically insignificant [Figure 4(a), Suppl
236 Figure 4(c)). In parallel cultures, *Mgat3* knockdown in S100β mVSCs resulted in a
237 significant reduction in lectin binding of immunoprecipitated Notch1 with both the ConA
238 and E-PHA lectins compared to the scrambled control, while no significant reduction in
239 binding was detected with LCA or WGA lectins [Figure 4(b)]. Meanwhile, *Fut8*
240 knockdown led to significant decreases in ConA and LCA binding, but not for WGA or E-
241 PHA lectins [Figure 4(b)].

242 The repercussions of *Mgat3* and *Fut8* knockdown on Jagged-1 induced Notch signalling
243 and myogenic differentiation revealed a significant reduction in Jagged-1 stimulated *Hey1*
244 and *Myh11* expression in S100β mVSCs and C3H10T1/2 cells following both *Mgat3*
245 knockdown [Figure 4(c), (d), Suppl Figure 5(c), (d)] and *Fut8* knockdown, respectively
246 [Figure 4(e), (f), Suppl Figure 5(e), (f)], when compared to the scrambled controls. In
247 contrast, Notch1 NICD induced Notch signalling and myogenic differentiation of S100β
248 mVSCs was unaffected by *Mgat3* [Figure 5(a), (b)] and *Fut8* knockdown [Figure 5(c),
249 (d)], when compared to the empty vector (EV) controls. Moreover, the decrease in *Hey1*
250 expression following *Fut8* knockdown in S100β mVSCs was not due to changes in the
251 expression of the Notch1 receptor as there was no significant change in either Notch1
252 protein expression [Figure 5(e, f)] or *Notch1* mRNA levels [Figure 5(g)] following
253 knockdown, compared to scrambled control. In contrast, while there was a slight albeit
254 significant change in the expression of Notch 1 protein levels following *Mgat3*
255 knockdown [Figure 5(e), (f)] this was not reflected in changes to *Notch1* mRNA levels
256 [Figure 5(g)].

257 **Inhibition of N-glycosylation impairs Notch receptor trafficking and degradation.**

258 N-glycosylation has been shown to be an essential modification for correct protein
259 trafficking from the endoplasmic reticulum (ER) and Golgi apparatus (GA) to their site of
260 action within the cell [50-51]. Therefore, the possibility that inhibition of N-glycosylation
261 by either chemical inhibitor (TNC or DMJ) or knockdown of *Mgat3* and *Fut8* interferes
262 with Notch1 protein trafficking and localisation to the membrane was explored.
263 Membrane fractionation of crude lysate from S100β mVSCs revealed the presence of
264 distinct protein band profiles between each fraction, confirmed using pan-cadherin, a
265 ubiquitously expressed membrane-bound protein [Figure 6(a)]. Fractionation revealed that
266 the transmembrane Notch1 protein is exclusively present in the membrane fraction and
267 absent in the cytosolic fraction [Figure 6(a)]. Following treatment of the cells with TNC
268 or DMJ for 48 h, there was a significant reduction in the expression of Notch1 in the
269 membrane fraction [Figure 6(b), (d)]. Brefeldin A (BFA), as a potent inhibitor of protein
270 transport in the Golgi apparatus, served as a positive control. Since cellular Notch1
271 protein levels remained unchanged following treatment with TNC and DMJ [Suppl Figure
272 3(c), (d)], it is unlikely that TNC and DMJ treatment was causing endocytosis and
273 degradation of the receptor [Figure 6(b)]. This observation was further supported by
274 immunocytochemical analysis of Notch1 localisation *in situ*. Golgin97 served as a control
275 to visualise the subcellular location of the GA [Figure 7(a),(c)]. The ratio of both the

fluorescence intensity and density significantly decreased following treatment with TNC, DMJ or BFA [Figure 7(c)] wherein a significant decrease in the ratio of membrane:perinuclear localisation of Notch1 was observed following treatment [Figure 7(a), (c)]. Lower ratios indicate a higher level of fluorescence in the perinuclear region compared to that at the membrane. This analysis suggests an accumulation of Notch1 in the perinuclear region of the cell in response to TNC and DMJ treatment, similar to BFA [Figure 7(a), (c)] and supports a significant reduction of Notch1 protein trafficking following inhibition of N-glycosylation.

In a similar manner, membrane fractionation was used to determine whether knockdown of *Mgat3* and *Fut8* also reduced Notch1 localisation to the membrane. There was a significant reduction in the expression of Notch1 in the membrane fraction following *Mgat3* knockdown, compared to the scrambled control. In contrast, there was no significant change following *Fut8* knockdown [Figure 6(c), (e)]. This analysis suggests that Notch1 trafficking from the GA to the plasma membrane is inhibited by *Mgat3* knockdown. However, in parallel experiments, immunocytochemical analysis of Notch1 localisation *in situ* following knockdown of *Mgat3* and *Fut8* demonstrated that there was no significant change in the ratio of either the fluorescence intensity or density following knockdown whereas both ratios decreased significantly following treatment BFA [Figure 7(b), (d)]. Therefore, it is more likely that this reduction is due to the decrease in total Notch1 protein in the cell following *Mgat3* knockdown [Figure 5(e)].

In summary, knockdown of the *GnT-III* and *Fut8* glycosyltransferases provided a more specific insight into how two groups of N-glycans (bisected and core fucosylated) contributed to Notch signalling and myogenic differentiation. Knockdown of the *Mgat3* transcript (which codes for the GnT-III protein) led to a reduction in E-PHA binding, while *Fut8* knockdown resulted in a decreased level of LCA binding. These findings provide evidence for the presence of both complex bisecting and core fucosylated N-glycans on the Notch1 receptor. Moreover, knockdown of *GnT-III* and *Fut8* glycosyltransferases demonstrated that both groups of N-glycans play a major role in activation of both Notch target gene expression and myogenic marker expression following Jagged-1 activation of mVSCs.

Site-directed mutagenesis of six N-glycosylation impairs Jagged-1 induced Notch signalling

Specific targeting of individual glycans to further define the function of both bisecting and core fucosylated N-glycans was performed through site-directed mutagenesis of the six N-glycosylation consensus sequences along the Notch1 ECD. Site-directed mutagenesis of plasmid-encoded Notch1 was chosen, and the proportion of transfected cells was maximised in each population through puromycin selection [Suppl Figure 6(a), (b)]. The optimum concentration of plasmid DNA was assessed using a green fluorescent protein (GFP)-coding plasmid [Suppl Figure 6(b)]. Using the *pCS2 Notch1 Full Length-6MT* plasmid, six single base substitutions were carried out separately on the Notch1 gene to alter asparagine residues at amino acid positions 888, 959, 1179, 1241, 1489 and 1587 to isoleucine residues. Mutant plasmids were sequenced and aligned with the wild- type plasmid sequence using Multalin to confirm that the correct single base substitution had been incorporated in each case. In each case an essential adenine base was correctly converted to a thymine base [Suppl Figure 7(a)]. Chromatograms were also generated to

321 determine the quality of both the sequencing read and the sample plasmid and confirmed
322 high quality with clearly defined peaks [Suppl Figure 7(b)].

323 Mutations at N888I, N1489I and N1587I all resulted in a significant decrease in ConA,
324 LCA and E-PHA binding compared to that observed in the wild-type cells but did not
325 significantly alter WGA binding. N959I led to a significant reduction only in ConA
326 binding, while N1179I caused a significant attenuation in only the binding of LCA [Figure
327 8(a)]. In parallel cultures, Jagged-1 significantly increased the expression of *Hey1* in
328 control wild-type Notch1 transfected cells, an effect that was significantly attenuated by
329 mutations N888I, N1241I and N1587I of the Notch1 ECD [Figure 8(b)] concomitant with
330 a significant reduction in Jagged-1 induced *Myh11* expression [Figure 8(b)].

331 The changes in *Hey1* or *Myh1*1 expression were not attributed to a discrepancy in
332 efficiency of plasmid transfection across mutants as there was no significant difference
333 between levels of Notch1-coding plasmid DNA across all mutant plasmid samples
334 compared to the wild-type control [Suppl Figure 8(a)]. However, a significant decrease in
335 Notch1 protein levels was observed in cells transfected with mutants N1241I and N1587I,
336 respectively, while no significant change was detected across all other mutants, compared
337 to the wild-type control [Figure 8(d)]

338 These data indicate that all the mutations incorporated into the Notch1 gene, except
339 N1241, had a measurable effect on receptor glycosylation. Lectin binding indicated the
340 presence of a range of different N-glycan structures on the Notch1 ECD, including core
341 fucosylated and bisecting N-glycans, and some additional structures that could not be
342 identified with the limited range of lectins used. Mutation of asparagine residues at
343 Notch1 N-glycosylation sites reduced *Hey1* expression (N888I, N1241I and N1587I) and
344 *Myh11* expression (all mutations) following Jagged-1 stimulation. This was not due to
345 altered plasmid transfection efficiency, but for some mutants (N1241I and N1587I),
346 altered expression and/or degradation of Notch1 may be involved. It is likely that the N-
347 glycans at the four other mutation sites may influence Notch1 processing and signalling,
348 such as receptor cleavage or trafficking.

349

350 **Discussion**

351 Glycosylation is an essential regulator of many cellular processes and Notch
352 signalling is no different [52]. In contrast to the well documented role of O-glycosylation,
353 very little is known about the structure and function of Notch1 N-linked glycans. Here we
354 report on bisecting and core fucosylated N-glycans decorating the extracellular domain
355 (ECD) of the Notch1 receptor and their putative role in ligand-induced Notch signalling
356 and myogenic differentiation of resident vascular stem cells *in vitro.*

357

358 O-glycosylation is well established as influencing the folding, trafficking,
359 activation, and cleavage of Notch1 [29, 53-55]. Although it has been shown that there are
360 six highly conserved N-glycosylation sites on the Notch receptor [31], there is currently
361 no data available to determine how many of these sites are glycosylated and what type of
362 N-glycans reside on the receptor, other than data that suggests the Notch1 receptor
363 contains complex bisecting N-glycans [56]. The Notch signalling pathway, and the
364 Notch1 receptor in particular, plays an important role in lineage specification *in vitro* and

365 vascular lesion formation *in vivo* [10, 22]. Therefore, this study sought to characterise the
366 profile of N-glycosylation of the Notch1 receptor and explore the impact of removing
367 these N-glycans on Notch signalling and on Notch-mediated myogenic differentiation of
368 S100β stem cells.

369

370 The Notch signalling pathway drives myogenic specification of a range of stem
371 cells, including S100β resident mVSCs [22-24, 42, 57]. Here, immobilised recombinant
372 Jagged-1 was used to activate the Notch receptor and stimulate the expression of both
373 Notch target genes and myogenic markers in S100β mVSCs. Canonical Notch signalling
374 operates via the NICD-RBP-Jκ complex which, along with other transcription factors,
375 activates Notch target gene expression [3]. The NICD-RBP-Jκ complex is essential for
376 maintaining SMC differentiation [48, 58] through interaction with the serum response
377 factor (SRF)-myocardin transcription activator complex [59]. However, several studies
378 have described the ability of Notch target genes, such as *Hey1* and *Hey2*, to inhibit
379 myocardin-induced SMC differentiation, although many of these studies differ in their
380 description of the mechanism of inhibition, with some citing a direct interaction between
381 Notch target genes and SRF, while others suggest that this occurs via an independent
382 parallel pathway [21, 60]. While it has been well documented that Notch target genes such
383 as *Hey1* and *Hes1* contain RBP-Jκ binding domains at specific GTGGGAA consensus
384 sequences within their promoter regions [61-62], bioinformatic analysis of the *Myh11* and
385 *Cnn1* promoter regions suggests this consensus sequence is also present within their
386 promoter [63]. Moreover, CBF1 (the human form of RBP-Jκ) interacts with SMAD2/3 in
387 the TGF-β signalling pathway to promote transcription of SMC genes independent of
388 myocardin, such as *Cnn1* and *SM22α,* albeit this interaction was not observed with
389 Notch1 [63]. While NICD induced Notch signalling in S100β mVSCs promotes Notch
390 target gene and myogenic gene expression in S100β mVSCs, the Jagged-1 response was
391 dependent on canonical Notch signalling as the γ-secretase inhibitor, DAPT effectively
392 abrogate this response.

393 Mammalian cells express four different types of Notch receptor (Notch1 - 4) and
394 each one can initiate downstream Notch signal transduction in target cells [64]. Notch1
395 plays a role in the process of arterial remodelling and lesion formation [8, 10, 49]. Here,
396 knockdown of *Notch1* mRNA in mVSCs using siRNA significantly attenuated Jagged-1-
397 induced Notch target gene and myogenic gene expression confirming the pivotal role of
398 Notch1 in lineage specification in these cells. Future studies that selectively delete the
399 Notch1 receptor in resident S100β mVSCs using *S100β-CreERT2* transgenic mice crossed
400 with Notch1 floxed mice before vascular injury will reveal the importance of this data *in*
401 *vivo,* in addition with studies that explore the role of the other three Notch receptors in this
402 process. In this context, loss of Notch 2 in SMCs leads to protein profile changes during
403 lesion formation but does not alter overall lesion morphology or cell proliferation [65].
404 Nevertheless, the current findings highlight the potential of Notch1 as a therapeutic target
405 for controlling the accumulation of SMC-like cells from mVSCs in arteriosclerotic lesion
406 progression.

407 To date, evidence regarding the profile of N-linked glycans on the Notch1 receptor
408 suggests that six consensus sites are present and highly conserved along the ECD, and that
409 at least some of the N-glycans at these sites contain a bisecting structure [31, 66]. In the
410 current study, ELLA analysis of the purified Notch1 receptor confirmed the presence of
411 N-glycans, and of bisecting N-glycans, whilst also revealing the existence of
412 oligosaccharides with a fucose residue bound to the core GlcNAc by an α-1,6 linkage

413 (referred to as core fucosylation). Treatment with global N-glycosylation inhibitors
414 tunicamycin (TNC) and 1-deoxymannojirimycin (DMJ) further supported these findings
415 as each inhibitor promoted a reduction in binding of the E-PHA (specific for bisecting
416 structures) and LCA (specific for core fucosylated structures) lectins to the purified
417 Notch1 protein. However, many lectins have weak affinity for oligosaccharide structures
418 other than their main binding target, including both E-PHA and LCA [67, 68]. To further
419 confirm the type of structures bound by these lectins, a strategy of siRNA knockdown was
420 implemented to inhibit the expression of the glycosyltransferases responsible for the
421 formation of bisecting and core fucosylated N-glycans, namely GnT-III and Fut8,
422 respectively.

423 Knockdown of the *Mgat3* and *Fut8* glycosyltransferase-coding genes reduced the
424 level of N-glycan structures on cellular glycoproteins within whole lysates. This includes
425 Notch1 as both knockdowns had a significant effect on bisecting or core fucosylated N-
426 glycans of the purified IP receptor, supporting the TNC and DMJ inhibition studies on the
427 presence of both bisecting and core fucosylated N-glycans decorating the Notch1 receptor.
428 *Mgat3* and *Fut8* knockdown reduced the level of ligand mediated Notch signalling and
429 myogenic differentiation in both mVSCs and C3H 10T1/2 cells. As downstream
430 components of Notch signalling and myogenic differentiation pathways following ectopic
431 expression of Notch1 NICD were not altered by *Mgat3* or *Fut8* knockdown, their effect
432 appears to be primarily on the Notch1 receptor as Notch pathway components downstream
433 of receptor cleavage were not affected by a reduction in synthesis of bisecting or core
434 fucosylated N-glycans. Furthermore, as Notch1 transcript levels were not affected by
435 either knockdown, but Notch1 protein expression was significantly reduced by *Mgat3*
436 expression, these data suggests that bisecting N-glycans may have a role in preventing the
437 degradation of the Notch1 receptor. The function of core fucosylated N-glycans is more
438 difficult to decipher as reduction of their synthesis through *Fut8* knockdown had no effect
439 on Notch1 protein expression or on receptor trafficking but caused a significant
440 attenuation of Notch signalling and myogenic differentiation. There may be an alternative
441 function for core fucosylated N-glycans on the Notch1 receptor, such as regulating
442 cleavage events.

443 However, as with the chemical inhibition strategies used in this study, this siRNA
444 knockdown strategy could also alter the N-glycosylation of proteins other than the Notch1
445 receptor and it is possible that this could influence Notch downstream signalling capacity.
446 Indeed, nicastrin, for example, is part of the γ-secretase complex which cleaves the NICD
447 from the Notch1 transmembrane domain (TMD) following receptor activation, and it
448 contains bisecting N-glycans which may be crucial for its role in the cleavage process [66,
449 69]. Similarly, *Fut9* knockdown of core fucosylated N-glycans impairs the proliferation
450 of S100β neural stem cells via inhibition of Musashi-1 (Msi-1), an RNA-binding protein
451 and activator of the Notch signalling pathway, that binds to *Numb* mRNA and inhibits its
452 translation. *Fut9* knockdown is coupled with increased Numb levels eventually resulting
453 in the suppression of Notch signalling [70]. Therefore, the reduction in Notch target gene
454 and myogenic gene expression following *Mgat3* and F*ut8* knockdown may have been due,
455 at least in part, to removal of N-glycans (bisected and core fucosylated) from other key
456 proteins impacting on Notch signalling in these cells. For this reason, it was important to
457 further explore the mechanisms by which core fucosylated and bisecting N-glycans were
458 affecting the Notch signalling process. Collectively, the data confirm a role for N-linked
459 bisecting glycosylation in the ligand activation of Notch1 in S100β mVSCs. Our finding
460 that inhibition of GnT-III blocks Notch activation suggests that targeting GnT-III or
461 blocking bisecting glycosylation sites on the Notch1 receptor may lead to new

462 therapeutics targeting neointimal formation. Overall, the evaluation of GnT-III expression
463 levels could also have clinical utility for stratifying patient cohorts that could benefit from
464 therapies that target Notch1 signalling.

465 The impact of N-linked glycosylation on O-fucose glycosylation of Notch is not
466 known. The N-linked sites within Notch1 ECD are in close proximity to O-fucose
467 modified sites. O-Fucose glycosylation of Notch EGF repeats has been shown to create a
468 code to either inhibit or activate Notch ligand-dependent activation [71]. It will be
469 important in the future to determine how the bisecting glycan structures on the Notch1
470 receptor in mVSCs alter this O-fucose code. While the importance of O-linked
471 glycosylation in Notch receptor-ligand binding and receptor processing and trafficking is
472 well documented [58, 60], little information is available on the role of N-glycans in this
473 context. While activation of Notch target genes by the ectopically expressed NICD was
474 not affected by TNC and DMJ, components of the myogenic differentiation pathway
475 downstream of Notch activation appeared altered leading to inhibition of that process.
476 These data did not necessarily implicate Notch1 N-glycosylation directly in the process, as
477 many other glycoproteins would be modified by the chemical inhibitors. However, further
478 investigation into how TNC and DMJ attenuated the Jagged-1 response revealed that it
479 was mediated by preventing Notch1 receptor trafficking out of the ER-Golgi complex to
480 the plasma membrane. A similar effect on Notch 3, where TNC treatment resulted in
481 accumulation of the receptor in the ER-Golgi complex has been reported [72]. While this
482 may be due to changes in glycosylation of the numerous proteins involved in receptor
483 trafficking, multiple previous reports have demonstrated that inhibiting the N-
484 glycosylation of developing proteins can block their transport to the membrane [73–75].
485 Therefore, it is likely that some of the N-glycans on the extracellular domain of the
486 Notch1 receptor are required for correct trafficking of the protein to the plasma
487 membrane. Unlike TNC and DMJ treatment, knockdown of GnT-III and Fut8 did not
488 affect downstream elements of either Notch signalling or myogenic differentiation
489 pathways, indicating that bisecting and core fucosylated N-glycans exert their influence on
490 the Jagged-1 response either at, or before, the point of Notch receptor activation. Analysis
491 of receptor trafficking revealed that inhibition of the glycosyltransferase did not result in
492 accumulation of Notch1 in the ER-Golgi complex, as was seen with chemical inhibition of
493 N-glycosylation. This suggests that the inhibition of trafficking observed following TNC
494 and DMJ treatment was either due to altered glycosylation of transport proteins or removal
495 of N-glycans on the Notch1 receptor which do not contain bisecting or core fucosylated
496 structures. Combination of receptor trafficking data and measurement of Notch1 protein
497 levels revealed that bisecting N-glycans prevent the accelerated degradation of the Notch1
498 receptor. This supports previous studies showing Notch1 receptor colocalization with
499 lysosomal degradation proteins following *Mgat3* knockdown [56]. The role of core
500 fucosylated N-glycans may be more directly related to the activation of the Notch1
501 receptor as knockdown of the *Fut8* glycosyltransferase inhibited Notch signalling and
502 myogenic differentiation but did not affect Notch1 expression, trafficking, degradation, or
503 downstream signalling.

504

505 Site-directed mutagenesis of the six N-glycosylation consensus sequences along
506 the Notch1 ECD further defined the function of both bisecting and core fucosylated N-
507 glycans. While initial analysis indicated that the amino acid site N1241 may not be
508 glycosylated, additional information indicates that it is more likely that the N-glycan at
509 this site was not detected due to the limited range of lectins used and the low binding
510 affinity of some lectins *in vitro* [76]. This is further emphasised by the fact that the N1179

511 mutation did not lead to a significant change in ConA binding, but did significantly reduce
512 the level of LCA binding, indicating that a core fucosylated oligosaccharide may be
513 present at this site which was not detected by ConA. Similarly, analysis of the N959
514 mutant indicated that an N-linked oligosaccharide is present at this site but does not
515 contain structures required for binding to LCA, WGA or E-PHA. Meanwhile, the glycan
516 at site N1179 was found to contain a core fucosylated structure. Finally, it is noteworthy
517 that N-glycans at N888, N1489 and N1587 shared a similar lectin binding profile with
518 significant reduction in the level of binding with ConA, LCA and E-PHA with these
519 mutants, suggesting that glycans at those sites are both core fucosylated and have a
520 bisecting structure. Therefore, it is possible that they share similar structural
521 characteristics and that the N-glycans at those sites may be both core fucosylated and have
522 a bisecting structure. However, this is unlikely as it has previously been demonstrated that
523 GnT-III modification of an oligosaccharide actively inhibits the addition of a fucose by
524 Fut8 [77]. This discrepancy may be explained by the alternative binding specificities of
525 certain lectins. E-PHA predominantly binds to N-glycans containing a bisecting structure
526 but has also been shown to have affinity for oligosaccharides with terminal galactose
527 residues [70,78]. Similarly, LCA has very high binding affinity for α1,6-fucosylated
528 glycans, but can also bind the mannose core of an N-glycan in the absence of 213 core
529 fucosylation [67]. Further investigation will be required to decipher which structures they
530 possess as data from the ELLA suggests the presence of either a core fucosylated N-
531 glycan with a possible terminal galactose residue, or a bisecting N-glycan. Data from
532 previous studies [56] along with glycosyltransferase knockdown and chemical inhibition
533 experiments in this study, suggests that at least one of these three sites contains an N-
534 glycan with a bisecting structure, with the most likely candidate being N1587 as mutation
535 of this residue resulted in the greatest reduction in E-PHA binding. Future studies using
536 additional mutations on both the essential asparagine residue and on other proximal non-
537 essential residues could reveal the impact of the amino acid alteration on protein
538 expression, function, and stability. Many studies which involve the mutation of N-
539 glycosylation sites on a glycoprotein also use simultaneous multi-site mutation to
540 investigate whether the combined impact of losing two or more N-glycans differs from the
541 effect observed following loss of a single N-glycan [75, 79, 80]. This is a strategy that
542 could reveal crucial information about the synergistic roles of N-glycans on the Notch1
543 ECD.

544 Regarding the mutations at sites N888, N1241 and N1587, their effect specifically
545 prevents canonical Notch signalling. ELLA data suggests that the N-glycan at N888
546 possessed either a bisecting or core fucosylated structure and combining this with
547 evidence from glycosyltransferase knockdown experiments, this means that its absence
548 does not lead to accumulation of Notch1 in the ER-Golgi complex. Furthermore, since the
549 mutation at this site did not result in any change to Notch1 protein levels in the cell, i.e.,
550 did not accelerate Notch1 degradation, this suggests that it is most likely a core
551 fucosylated N-glycan (possibly with a terminal galactose residue), rather than a bisecting
552 N-glycan. Taken together, these data suggest that the N-glycan at N888 has a direct
553 influence on Notch1 signal activation at the membrane. This may occur through regulation
554 of processes such as receptor folding or cleavage, mechanisms which are regularly
555 affected by loss of an individual N-glycan on other membrane-bound proteins [81-83].
556 The N1241I mutation resulted in a dramatic decrease in Notch1 protein levels in the cell,
557 implying that the Notch1 receptor was rapidly degraded, and as a result, Notch target gene
558 expression was inhibited. ELLA data suggested that there may have been no N-glycan
559 present at N1241 but evidence from this mutation experiment is a strong indication that an

560 N-glycan does indeed reside at this site but does not contain bisecting or core fucosylated
561 structures. Removal of the N-glycan at N1587 also reduced Notch1 protein levels, most
562 likely through receptor degradation. Combined with ELLA data and evidence from siRNA
563 knockdown experiments, the cumulative data suggests that the oligosaccharide which
564 resides at this site contains a complex bisecting structure.

565 Notably, all six mutations resulted in a reduction of the myogenic differentiation of
566 stem cells in response to Jagged-1 stimulation. This further supports lectin binding data by
567 confirming that N-glycans reside at each of the six consensus sites and reinforces data
568 from chemical inhibition and glycosyltransferase knockdown experiments by
569 demonstrating that all these glycans are involved in the process of Notch-mediated
570 myogenic differentiation. However, only the mutations at sites N888, N1241 and N1587
571 significantly attenuated the expression of the Notch target gene *Hey1*, suggesting that the
572 other three mutations at sites N959, N1179 and N1489 have an indirect effect on
573 myogenic differentiation which is independent of canonical Notch signalling. In addition,
574 none of these three mutations led to significant changes in Notch1 receptor protein levels
575 in the cell. Their effect on myogenic differentiation may be related to non-canonical Notch
576 signalling pathways, such as the Wnt/β-catenin pathway [84-86]. The Notch1 receptor has
577 been shown to interact with activated β-catenin at the membrane [87]. While this
578 interaction occurs at the intracellular C- terminal of the Notch1 receptor and it is unlikely
579 that any direct interaction takes place between these glycans and β-catenin, it is possible
580 that their absence leads to altered processing/folding of the receptor which results in
581 dysregulation of Wnt signalling and myogenic differentiation (Table II).

582 Data limitations include the narrow range of available lectins which are specific
583 for N-linked oligosaccharides. Most commercially available lectins exhibit their highest
584 affinity for a particular monosaccharide in a specific branching/linkage format. However,
585 many of these structures can be found in both O-linked and N-linked glycans, such as
586 Erythrina critagalli lectin (ECL) that bind strongly to the terminal galactose of an N-
587 acetyllactosamine-containing N-glycan, but will also bind to a terminal β1,4-galactose in
588 O-glycans [88]. In addition, while mutation of specific asparagine residues is a highly
589 specific method, a single change in nucleotide or amino acid sequence can have a dramatic
590 effect on the expression, processing and/or function of the target protein [80, 89]. In this
591 study, isoleucine was chosen as the substitute due the ease of mutation (only a single base
592 substitution required for each Asn site) and the non-reactive nature of the side chain.
593 However, the change in side-chain composition may alter the conformation of the receptor
594 or result in issues with steric hindrance [90]. While glutamine as a substitute is widely
595 used since its structure is the most similar to asparagine, the polar amide group of the
596 glutamine residue may lead to unwanted molecular reactions [91]. This can be
597 circumvented by mutating the Asn residue to a number of different amino acids, mutating
598 the serine/threonine residue in the consensus sequence, or mutating a proximal amino acid
599 which is not part of the consensus sequence [92]. Finally, alternative chemical inhibitors
600 such as swainsonine, which blocks α-mannosidase-II activity, could provide greater
601 insights into the role of N-glycans while knockdown of additional glycosyltransferases
602 such as GnT-IV and ST3Gal1 could be useful in deciphering the exact structures of N-
603 linked oligosaccharides on the Notch1 receptor [52, 93].

604 In conclusion, activation of the Notch1 receptor by its ligand, Jagged-1, stimulates
605 myogenic differentiation of resident S100β mVSCs. Furthermore, N-glycosylation
606 intervention strategies, including chemical inhibition, siRNA knockdown of the GnT-III
607 and Fut8 glycosyltransferases, and site-directed mutagenesis of N-glycosylation sites,
608 reveal that this signalling is heavily regulated by N-glycans which reside at six consensus

609 sequences along the extracellular domain of Notch1. Several key oligosaccharides at
610 these sites were found to contain bisecting or core fucosylated structures. Notch1
611 expression and trafficking analysis indicated that N-glycans at asparagine (N) 1241 and
612 1587 protect the receptor from accelerated degradation, while the oligosaccharide at N888
613 directly affects signal transduction. Conversely, N-linked glycans at the other three sites
614 do not impact canonical Notch1 signalling but still play a role in Notch-mediated
615 myogenic differentiation, possibly via a non-canonical Notch signalling pathway.

616 The putative role of bisecting and core fucosylated N-glycans in ligand induced
617 activation of the Notch1 receptor may present as a novel therapeutic target for controlling
618 Notch1 signalling and myogenic differentiation of S100β resident vascular stem cells
619 during subclinical atherosclerosis where these cells have been reported to play a major
620 role in early lesion development [16-18].
621

622 **Materials and Methods**

623

624 *Materials*

625

626 A full list of the materials is available in Supplementary Materials

627

628 *Cell Culture*

629

630 Cells were grown in tissue culture flasks (25-175 cm^2) or in 6-well plates in a humidified
631 incubator and were visualised by a Nikon Eclipse TS100 phase contrast microscope.
632 S100β mouse vascular stem cells (mVSCs) were isolated from the aortic arch of female
633 C57BL/6J mice (used in accordance with EU legislation (Directive 2010/63/EU)) as
634 previously described and grown in maintenance medium (MM1) containing DMEM
635 supplemented with 2% chick embryo extract, 1% FBS, 0.02 µg/ml, bFGF basic protein, B-
636 27 Supplement, N-2 supplement, 1% Penicillin-Streptomycin, 50 nM 2-Mercaptoethanol
637 and 100 nM retinoic acid [16]. These stem cells exhibited a uniform neural-like
638 morphology in low density culture adopting a dendritic-like tree shape and retaining their
639 morphological characteristics at low density throughout repeated passage. Cells were fed
640 with MM1 every 2-3 days and passaged every 3-4 days or when ~70% confluent. Cells
641 were routinely grown in MM and dissociated with 0.5X TrypLE and expanded. Cells were
642 used at passage numbers below p25. C3H/10T1/2 embryonic fibroblasts have been
643 extensively characterised as multipotent mesenchymal cells [47]. Clone 8 - CCL-226 cells
644 were grown in EMEM basal media supplemented with 10% heat inactivated FBS and 1%
645 Penicillin Streptomycin. Cells were used at passage numbers below P20 and were always
646 sub-cultured before confluency surpassed 70% to prevent post-confluence inhibition.
647 Freezing media consisted of EMEM with 10% FBS, 1% Pen-Strep and 5% DMSO.

648

649 *Adipogenesis Differentiation*

650

651 Adipogenic differentiation of mVSCs was performed using StemPro® adipogenesis
652 differentiation medium in accordance with the manufacturer's recommendations. Briefly,
653 cells were seeded at a density of 1 x 10^4 cells/cm^2 in their maintenance medium and left
654 for two days before being washed with PBS twice followed by feeding with StemPro®
655 adipogenesis differentiation media for 14 days. Cells were harvested and adipogenic
656 differentiation was evaluated by measuring the expression level of lipoprotein lipase (*Lpl*)
657 and fatty acid binding protein 4 (*Fabp4*).

Osteogenesis Differentiation

Osteogenic differentiation of mVSCs was performed using the StemPro® osteogenic differentiation medium in accordance with the manufacturer's recommendations. Briefly, cells were seeded at a density of 1 x 10^4 cells/cm^2 in their maintenance medium and left for two days before being washed with PBS twice followed by feeding with StemPro® osteogenic differentiation media for 21 days. Cells were harvested and osteogenic differentiation was evaluated by measuring the expression level of alkaline phosphatase (*Alpl*) and Sclerostin (*Sost)*.

Telomerase Activity Assay

Cell lysates were prepared using the RIPA buffer method and diluted to a protein concentration of 10-750 ng/µL before telomerase activity was measured using a TRAPeze® XL Telomerase Detection Kit. Briefly, PCR was carried out using fluorescein-labelled primers to amplify telomeric repeats in the sample DNA. Higher telomerase activity meant that there were more telomeric repeats to be amplified by the Taq polymerase, resulting in a more fluorescent product. The PCR products were analysed in a Tecan Safire II fluorescent plate reader. Telomerase activity was calculated by comparing the level of fluorescence detected in each sample to a standard curve generated from a set of telomeric repeat standards. The telomerase activity of a sample was given in TPG units.

Plasmid Amplification and Purification

Transformation: LB Agar (20g/L LB, 12g/L Agar) was made up in dH_2O and autoclaved to sterilise. After cooling to 55ºC, appropriate antibiotics were added (ampicillin at 100µg/mL or kanamycin at 50µg/mL). The agar was poured into sterile petri dishes, allowed to harden, and stored at 4ºC. A sample (100ng) of plasmid DNA was mixed with 50µL of competent JM109 bacterial cells in a sterile microfuge tube. Tube was placed on ice for 30 mins. Cells were then heat-shocked at 42ºC for 45 secs to allow plasmid DNA to cross the cell membrane. Tube was placed back on ice for 2 mins. 500µL of SOC medium (20% tryptone, 5% yeast extract, 0.5% NaCl, 1% 0.25M KCl, 2% 1M glucose) was added to the tube which was then incubated at 37ºC for 45 mins. The contents of the tube were transferred to a LB Agar plate with appropriate antibiotics. Plates were incubated overnight at 37ºC. A single colony was picked from the transformation plate and inoculated in 5mL of LB broth (20g/L LB) with appropriate antibiotics. This culture was incubated at 37ºC in a shaking incubator for 6-8 hours. 1.2mL of this culture was then transferred to a sterile conical culture flask containing 250mL of LB broth with appropriate antibiotic. Flask was incubated at 37ºC overnight in a shaking incubator. 50mL was removed from the flask for plasmid purification. The rest was used to make stocks by supplementing with 50% glycerol and storing at -80ºC.

Plasmid DNA Purification

Plasmid DNA was purified from transformed bacterial cells using the Invitrogen PureLink™ HiPure Plasmid Filter Midiprep Kit according to the manufacturer's guidelines. A Nanodrop® ND-1000 Spectrophotometer was used to quantitate the DNA concentration before DNA samples were interrogated by agarose gel electrophoresis and visualised with the SynGene G-Box.

RNA Extraction

RNA was extracted from cells using the Promega Reliaprep™ RNA Miniprep System according to the provided instructions. A Nanodrop® ND-1000 Spectrophotometer was used to quantitate the RNA concentration before RNA samples were analysed by *Quantitative Reverse-Transcription Polymerase Chain Reaction (qRT-PCR)*

Quantitative Reverse-Transcription Polymerase Chain Reaction (qRT-PCR)

Quantitative RT-PCR was performed using the Rotor Gene Q from Corbett Research, as previously described [16]. A ubiquitously expressed reference gene, hypoxanthine guanine phosphoribosyltransferase (*Hprt)* was used as a control. Two different kits were used for this method depending on the primer set: Rotor-Gene SYBR® Green RT-PCR Kit (Qiagen, 204174) and SensiFAST™ SYBR® No-ROX One-Step Kit (BioLine, BIO-72001). Samples were run in triplicate for each primer set.

Immunocytochemistry

Immunocytochemical analysis of protein expression in cells was performed, as described previously [16]. Fixed cells on coverslips were stained for expression of the intermediate myogenic differentiation marker Calponin1 (Cnn1) and the calcium binding protein, S100β by incubating overnight at 4ºC with antibody diluted to an appropriate concentration with 1% BSA in PBS. Cells were washed x3 and incubated at room temperature for 1 hr with the secondary antibody (diluted with 1% BSA in PBS), protected from light. Nuclear staining was performed with DAPI which was diluted to 1µg/mL. Coverslips were mounted before cell nuclei and antibody staining was visualised and imaged using the Olympus DP-50 fluorescent microscope. The number of positive cells was counted for each image and divided by the total number of cells in that image to give a ratio, and subsequently a percentage, of antigen-positive cells.

Transient Transfections

Transfection of both plasmid DNA and single strand siRNA duplexes into cells was performed using the Mirus Bio TransIT-X2® dynamic delivery system, according to the manufacturer's guidelines after optimization. Cells were grown to ~ 80% confluency in the maintenance medium before transfection. The transfection mix was made up in a sterile microfuge tube according to kit protocol and incubated at room temperature for 30 minutes to allow transfection complexes to form. This mixture was then added dropwise to the cell culture. Cells were incubated at 37ºC for 48 hours before harvesting. Transfection efficiency was assessed using a control GFP-plasmid or TYE 563 DsiRNA (Mirius Bio), a fluorescently tagged siRNA. A non-transfected sample was used as a negative control. Cells were incubated at 37ºC for 48 h before being fixed with 3.7% formaldehyde. Nuclei were stained with DAPI, and coverslips were mounted onto slides before being imaged using a Olympus DP-50 fluorescent microscope. The number of cells containing GFP, or dye were counted and graphed as a percentage of the total number of cells. A transfection efficiency of 99.6% was achieved in the dye-transfected sample, compared to 0% in the non-transfected sample.

758 *Genomic DNA Extraction*
759
760 Genomic DNA was extracted from cells using the Bioline ISOLATE II Genomic DNA Kit
761 according to the manufacturer's instructions. Briefly, cells were washed and scraped into
762 PBS and pelleted by centrifugation at 1500 rpm for 5 minutes. The pellet was resuspended
763 in lysis buffer GL. Proteinase K and Lysis Buffer G3 were then added to the sample
764 before incubation at 70ºC for 15 minutes. 99% ethanol was added to each sample to adjust
765 DNA binding conditions. Samples were loaded into columns containing a silica membrane
766 and centrifuged at 11,000 x g for 1 minute. The flow-through was discarded and columns
767 were washed twice in wash buffer. Elution buffer was then added to each column.
768 Samples were incubated at room temperature for 1 minute before centrifugation at 11,000
769 x g for 1 minute. The flow-through contained the purified DNA.
770
771 *Protein Isolation and Quantitation*
772
773 Cells at >80% confluency were scraped into culture media and pelleted by centrifugation.
774 The supernatant was discarded, cells were resuspended in an appropriate volume of RIPA
775 buffer and incubated on ice for 30 minutes to induce cell lysis. The lysate was then
776 clarified by centrifugation at 8,000 x g for 20 minutes at 4ºC. The supernatant containing
777 cellular proteins was retained while the cell debris pellet was discarded. The Pierce™
778 BCA Protein Assay Kit was used to quantitate the concentration of protein in the clarified
779 cell lysate.
780
781 *Membrane Protein Isolation*
782
783 Isolation of proteins from the cell membrane was carried out using the Mem-PER Plus
784 Membrane Protein Extraction Kit according to the manufacturer's instructions.
785
786 *Membrane Fractionation*
787
788 Cells were harvested and the Mem-PER™ Plus Membrane Protein Extraction Kit was
789 used to perform membrane fractionation on the crude lysate according to the
790 manufacturer's instructions. Protein concentration in both the cytoplasmic fraction and
791 membrane fraction was quantified by BCA Assay. Both samples were run on an SDS-
792 PAGE precast protein gel and subsequently transferred to a nitrocellulose membrane.
793 Staining with Ponceau S confirmed the difference in the presence of protein band profiles
794 between the two samples. Immunoblotting was then carried out with an anti-Notch1
795 antibody and chemiluminescent staining was used to visualise bands.
796
797 *Effect of TNC and DMJ on Membrane Localisation of Notch1*
798
799 Cells were treated in the absence or presence of TNC (0.5µg/mL), DMJ (4µg/mL), 1 x
800 Brefeldin A (BFA) at 37ºC for 48 h before being harvested. Membrane fractions were
801 isolated using the Mem-PER™ Plus Membrane Protein Extraction Kit, according to the
802 manufacturer's instructions. Protein concentration in the membrane fractions was
803 measured by BCA Assay. Western blot was then carried out and samples were immuno-
804 probed using an anti-Notch1 antibody. Chemiluminescent staining was used to visualise
805 immunoblotting. Densitometry was carried out using ImageJ to measure the intensity of
806 Notch1 bands while β-actin, pan-cadherin and Ponceau S staining was used as loading
807 controls.

808
809 *Trafficking of Notch1 Receptor*
810
811 Cells were seeded at 5,000 cells/well onto sterile coverslips and treated with or without
812 TNC (0.5µg/mL), DMJ (4µg/mL), 1 x BFA at 37ºC for 48 h before being fixed with 3.7%
813 formaldehyde. Immunocytochemistry was then carried out and cells were stained using an
814 anti-Notch1 antibody with an IgG control antibody used as a secondary control. A control
815 sample was also stained with an anti-Golgin-97 antibody to visualise the subcellular
816 location of the golgi apparatus (GA). Nuclei were stained with DAPI. Samples were
817 imaged using a fluorescent microscope. ImageJ was used to calculate the mean
818 fluorescence intensity and the integrated density of fluorescence at both the cell membrane
819 and in the perinuclear region (adjacent to the nucleus, i.e., where the GA is located).
820 Samples were graphed as a ratio of the fluorescence at the membrane to the fluorescence
821 in the perinuclear region.
822
823
824 *Purification of Notch1 by Immunoprecipitation*
825
826 Protein lysates were prepared, and the protein concentration measured by BCA assay.
827 Immunoprecipitation was carried out using Protein A-conjugated magnetic beads and
828 either an anti-Notch1 rabbit monoclonal antibody, a rabbit IgG control antibody, or a
829 mouse IgG control antibody. Following incubation with the antibody, supernatants
830 (containing unbound proteins) were transferred to a fresh tube and appropriately stored.
831 Bound protein was eluted off the beads by either 1X Laemmli Buffer or a 0.1M Glycine
832 buffer (pH 2.0). Samples eluted with the glycine buffer were neutralised using a 1M Tris
833 buffer (pH 9.0). Both eluted bound proteins and previously stored unbound protein
834 samples were then run on an SDS-PAGE precast protein gel, transferred to a nitrocellulose
835 membrane, immuno-probed using an anti-Notch1 antibody and visualised by TMB
836 staining of the HRP-conjugated secondary antibody.
837
838 *Ectopic Expression of Myc-tagged Notch1 and NICD*
839
840 The pCS2 Notch1 full length-6MT and pCS2 Notch1 ICv-6MT plasmids were purchased
841 from Addgene (LGC Standards, Teddington, UK) as bacterial stabs. Plasmid-containing
842 bacteria were transferred to a 5mL culture with selective antibiotic at 37ºC for 8 hrs.
843 1.2mL of this culture was then transferred to a 250mL secondary culture with selective
844 antibiotics which was incubated overnight at 37ºC. Plasmid DNA was isolated from this
845 culture using the Invitrogen PureLink^{TM} HiPure Plasmid Filter Midiprep Kit. To verify
846 plasmid length and quality, plasmid DNA was digested with an appropriate restriction
847 enzyme. This served to linearise the DNA before running plasmid samples through gel
848 electrophoresis on an agarose gel. Visualisation of this gel under UV light confirmed that
849 plasmids were the correct length and that the stocks contained no contaminating DNA. To
850 validate the ectopic expression of both proteins, cells were grown to ~80% confluency in 3
851 wells of a 6-well plate and transfected with either the Notch1 full-length plasmid, the
852 NICD plasmid or an empty vector plasmid (pCDNA3.1) using the TransIT-X2 Dynamic
853 Delivery System. Cells were incubated at 37ºC for 48 h in MM1 before being harvested.
854 Protein was isolated and quantified by BCA assay. Western blot was then carried out, with
855 all samples being immuno-probed using an anti-Myc-tag antibody to stain for either the
856 myc-tagged Notch1 or myc-tagged NICD, and an anti-β-actin antibody was used as the
857 loading control.

858
859 *Western Blot*
860
861 Following protein isolation and quantitation, samples were prepared for SDS-PAGE using
862 a precast SDS 10% polyacrylamide gel to perform electrophoresis and the Pierce™ G2
863 Fast Blotter for protein transfer, as previously described [48]. Ponceau S staining
864 confirmed that the transfer had been successful. Blocking buffer (5% dried milk in TBS
865 with 0.1% Tween) was added to the membrane and incubated at room temperature for 1-2
866 h on a rocker before the membrane was washed in TBST (50mM Tris, 150mM NaCl,
867 1mM $MnCl_2$, 1mM $CaCl_2$, 1mM $MgCl_2$, 0.1% Tween-20) and incubated with the primary
868 antibody (diluted with 5% BSA in TBST) overnight on a rocker at 4ºC. Primary antibody
869 was removed, membrane washed 3 times (5 minutes each) with TBST, before incubation
870 with an HRP-conjugated secondary antibody (diluted with 5% BSA in TBST) on a rocker
871 for 1 hr at room temperature. Fresh TMB was added to the membrane which was then
872 incubated on a rocker at room temperature for approx. 10 mins before the blot was imaged
873 using BioRad GelDoc EZ Gel System. Alternatively, Pierce™ ECL Western Blotting
874 Substrate was added to the membrane which was then incubated on a rocker at room
875 temperature for 5 minutes. The blot was then imaged using Syngene G-Box.
876
877 *Enzyme-Linked Lectin Assay (ELLA)*
878
879 All samples were diluted to the same concentration with 50µL of treated sample or control
880 sample added in triplicate to each well of a 96-well plate. The plate was incubated
881 overnight at 4ºC with gentle shaking. Wells were emptied and blocking buffer (0.5% PVA
882 in PBS) added to each well. The plate was incubated for 2 hrs at room temperature with
883 gentle shaking before wells were washed with TBST (50mM Tris, 150mM NaCl, 1mM
884 $MnCl_2$, 1mM $CaCl_2$, 1mM $MgCl_2$, 0.1% Tween-20). Biotinylated lectins (50µL, 5µg/mL)
885 were added to each well and incubated at room temperature for 1 hr with gentle shaking
886 before wells were emptied and washed again with TBST. HRP-conjugated anti-biotin
887 antibody (50µL, 1:10,000) was then added to each well and incubated at room temperature
888 for 1 hour with gentle shaking. Wells were washed with TBST before a TMB substrate
889 solution (90µL) was added and incubated for 10 minutes at room temperature with gentle
890 shaking. Stop solution (10% H_2SO_4) was added to each well before the absorbance was
891 measured at 450 nm in a plate reader.
892
893 *N-glycosylation Profile of Purified Notch1*
894
895 Cells were grown to ~80% confluency in 3 wells per 6-well plate. One well was not
896 transfected while the TransIT-X2 Dynamic Delivery System was used to transfect the
897 other two wells with either the Notch1 full-length plasmid or an empty vector control
898 plasmid. Cells were incubated at 37ºC for 48 h in maintenance media (MM1) before being
899 harvested. Protein was isolated and quantified by BCA assay. IP was carried out to purify
900 the ectopically expressed Notch1 using Protein G-conjugated magnetic beads and an anti-
901 Myc-tag antibody. The non-transfected sample was immunoprecipitated with a mouse IgG
902 control antibody. Bound proteins were eluted off the magnetic beads using a 0.1M Glycine
903 buffer (pH 2.0) and a 1M Tris buffer (pH 9.0) was used to neutralise the purified protein
904 fraction. BCA assay was carried out again to determine the concentration of protein in
905 each sample post-IP. ELLA was then applied to detect the presence of N-glycans in all
906 three samples. Control wells containing PBS rather than a protein sample were used to
907 determine the baseline for non-specific absorbance, while the mouse IgG control sample

acted as the baseline for non-specific lectin- or antibody-binding to the IP eluate. Both baseline values were subtracted from sample absorbance values to decipher the true level of specific lectin binding. TBST acted as the vehicle control for all lectins.

Site-directed mutagenesis

Mutation of N-glycosylation sites on a plasmid-encoded Notch1 receptor was achieved using the Agilent QuikChange Lightning Site Directed Mutagenesis Kit, according to the manufacturer's instructions. Briefly, primers were specific for a region of the Notch1 gene containing an N-glycosylation site and were designed to incorporate a single base substitution in copies of the plasmid DNA template. PCR tubes were placed in an Applied Biosystems® Veriti® Thermal Cycler. A DpnI restriction enzyme was added to each tube of PCR products to degrade any parental template DNA. Mutant plasmids were then transformed into ultracompetent XL10-Gold bacterial cells via heat-shock at 42ºC. After allowing the cells to recover for 1 hour in NZY^+ broth at 37ºC, each transformation reaction was spread on an LB agar plate with Ampicillin (50µg/mL) and incubated at 37ºC overnight. Colonies were picked and inoculated in liquid LB. Transformed bacteria were grown and mutant plasmids were purified before sending them for sequencing with Source Biosciences to confirm that the correct single base substitution had been incorporated in each case.

Data Analysis and Statistics

The mean and standard deviation (or standard error margin) was calculated for all the technical and biological replicates in each experiment and these values were used to plot the data. The Kolmogorov-Smirnov normality test was used to analyse the spread of the data as it uses the most stringent conditions. The outcome of the normality test (along with the number of samples and parameters) dictated what type of significance test was carried out. In the case of data containing only two samples, an unpaired t-test with Welch's correction was performed on normally distributed data. For non-parametric (skewed) data, the Wilcoxon test was carried out to calculate statistical significance. For data containing more than two samples, ANOVA testing was used to perform multiple comparisons between all samples. This could be carried out using an ordinary one-way (one parameter to compare) or two-way (two parameters to compare) ANOVA for normalised data, or the Kruskal-Wallis test for non-parametric data. This would reveal the level of statistical significance for both the data as a whole and between each sample.
The Materials and Methods section should provide sufficient information to allow replication of the results. Begin with a section titled Experimental Design describing the objectives and design of the study as well as prespecified components.

References

1. MacGrogan D, Münch J, de la Pompa JL. Notch and interacting signalling pathways in cardiac development, disease, and regeneration. Nat Rev Cardiol. 2018;15:685–704.
2. Talora C, Campese AF, Bellavia D, Felli MP, Vacca A, Gulino A, et al. Notch signaling and diseases: an evolutionary journey from a simple beginning to complex outcomes. Biochim Biophys Acta. 2008;1782:489–97.
3. Bray SJ. Notch signalling in context. Nat Rev Mol Cell Biol. 2016;17:722–35.

957 4. Siebel C, Lendahl U. Notch Signaling in Development, Tissue Homeostasis, and Disease.
958 Physiol Rev. 2017;97:1235–94.

959 5. Katoh M. Canonical and non-canonical WNT signaling in cancer stem cells and their
960 niches: Cellular heterogeneity, omics reprogramming, targeted therapy and tumor plasticity
961 (Review). Int J Oncol. 2017;51:1357–69.

962 6. Caolo V, Schulten HM, Zhuang ZW, Murakami M, Wagenaar A, Verbruggen S, et al.
963 Soluble Jagged-1 inhibits neointima formation by attenuating Notch-Herp2 signaling.
964 Arterioscler Thromb Vasc Biol. 2011;31:1059–65.

965 7. Lindner V, Booth C, Prudovsky I, Small D, Maciag T, Liaw L. Members of the
966 Jagged/Notch gene families are expressed in injured arteries and regulate cell phenotype via
967 alterations in cell matrix and cell-cell interaction. Am J Pathol. 2001;159:875–83.

968 8. Li Y, Takeshita K, Liu P-Y, Satoh M, Oyama N, Mukai Y, et al. Smooth muscle Notch1
969 mediates neointimal formation after vascular injury. Circulation. 2009;119:2686–92.

970 9. Sakata Y, Xiang F, Chen Z, Kiriyama Y, Kamei CN, Simon DI, et al. Transcription factor
971 CHF1/Hey2 regulates neointimal formation in vivo and vascular smooth muscle
972 proliferation and migration in vitro. Arterioscler Thromb Vasc Biol. 2004;24:2069–74.

973 10. Redmond EM, Liu W, Hamm K, Hatch E, Cahill PA, Morrow D. Perivascular delivery of
974 Notch 1 siRNA inhibits injury-induced arterial remodeling. PLoS One. 2014;9:e84122.

975 11. Chappell J, Harman JL, Narasimhan VM, Yu H, Foote K, Simons BD, et al. Extensive
976 Proliferation of a Subset of Differentiated, yet Plastic, Medial Vascular Smooth Muscle
977 Cells Contributes to Neointimal Formation in Mouse Injury and Atherosclerosis Models.
978 Circ Res. 2016;119:1313–23.

979 12. Dobnikar L, Taylor AL, Chappell J, Oldach P, Harman JL, Oerton E, et al. Disease-relevant
980 transcriptional signatures identified in individual smooth muscle cells from healthy mouse
981 vessels. Nat Commun. 2018;9:4567.

982 13. Majesky MW, Horita H, Ostriker A, Lu S, Regan JN, Bagchi A, et al. Differentiated Smooth
983 Muscle Cells Generate a Subpopulation of Resident Vascular Progenitor Cells in the
984 Adventitia Regulated by Klf4. Circ Res. 2017;120:296–311.

985 14. Kramann R, Goettsch C, Wongboonsin J, Iwata H, Schneider RK, Kuppe C, et al.
986 Adventitial MSC-like Cells Are Progenitors of Vascular Smooth Muscle Cells and Drive
987 Vascular Calcification in Chronic Kidney Disease. Cell Stem Cell. 2016;19:628–42.

988 15. Wan M, Li C, Zhen G, Jiao K, He W, Jia X, et al. Injury-activated transforming growth
989 factor β controls mobilization of mesenchymal stem cells for tissue remodeling. Stem Cells.
990 2012;30:2498–511.

991 16. Di Luca M, Fitzpatrick E, Burtenshaw D, Liu W, Helt J-C, Hakimjavadi R, et al. The
992 calcium binding protein S100β marks hedgehog-responsive resident vascular stem cells
993 within vascular lesions. NPJ Regen Med. 2021;6:10.

994 17. Molony C, King D, Di Luca M, Kitching M, Olayinka A, Hakimjavadi R, et al. Disease-
995 Relevant Single Cell Photonic Signatures Identify S100β Stem Cells and their Myogenic
996 Progeny in Vascular Lesions. Stem Cell Rev Rep. 2021;17:1713–40.

997 18. Yuan F, Wang D, Xu K, Wang J, Zhang Z, Yang L, et al. Contribution of Vascular Cells to
998 Neointimal Formation. PLoS One. 2017;12:e0168914.

999 19. Tang J, Wang H, Huang X, Li F, Zhu H, Li Y, et al. Arterial Sca1+ Vascular Stem Cells
1000 Generate De Novo Smooth Muscle for Artery Repair and Regeneration. Cell Stem Cell.
1001 2020;26:81-96.e4.

1002 20. Lyu L, Li Z, Wen Z, He Y, Wang X, Jiang L, et al. Fate mapping RNA-sequencing reveal
1003 Malat1 regulates Sca1+ progenitor cells to vascular smooth muscle cells transition in
1004 vascular remodeling. Cell Mol Life Sci. 2023;80:118.

1005 21. Proweller A, Pear WS, Parmacek MS. Notch signaling represses myocardin-induced smooth
1006 muscle cell differentiation. J Biol Chem. 2005;280:8994–9004..

1007 22. Kurpinski K, Lam H, Chu J, Wang A, Kim A, Tsay E, et al. Transforming growth factor-
1008 beta and notch signaling mediate stem cell differentiation into smooth muscle cells. Stem
1009 Cells. 2010;28:734–42.

1010 23. Doi H, Iso T, Sato H, Yamazaki M, Matsui H, Tanaka T, et al. Jagged1-selective notch
1011 signaling induces smooth muscle differentiation via a RBP-Jkappa-dependent pathway. J
1012 Biol Chem. 2006;281:28555–64.

1013 24. High FA, Zhang M, Proweller A, Tu L, Parmacek MS, Pear WS, et al. An essential role for
1014 Notch in neural crest during cardiovascular development and smooth muscle differentiation.
1015 J Clin Invest. 2007;117:353–63.

1016 25. Kopan R, Ilagan MXG. The canonical Notch signaling pathway: unfolding the activation
1017 mechanism. Cell. 2009;137:216–33.

1018 26. Fortini ME. Notch signaling: the core pathway and its posttranslational regulation. Dev Cell.
1019 2009;16:633–47.

1020 27. Matsumoto K, Luther KB, Haltiwanger RS. Diseases related to Notch glycosylation. Mol
1021 Aspects Med. 2021;79:100938.

1022 28. Moloney DJ, Shair LH, Lu FM, Xia J, Locke R, Matta KL, et al. Mammalian Notch1 is
1023 modified with two unusual forms of O-linked glycosylation found on epidermal growth
1024 factor-like modules. J Biol Chem. 2000;275:9604–11.

1025 29. Acar M, Jafar-Nejad H, Takeuchi H, Rajan A, Ibrani D, Rana NA, et al. Rumi is a CAP10
1026 domain glycosyltransferase that modifies Notch and is required for Notch signaling. Cell.
1027 2008;132:247–58.

1028 30. Shao L, Moloney DJ, Haltiwanger R. Fringe modifies O-fucose on mouse Notch1 at
1029 epidermal growth factor-like repeats within the ligand-binding site and the Abruptex region.
1030 J Biol Chem. 2003;278:7775–82.

1031 31. Takeuchi H, Haltiwanger RS. Significance of glycosylation in Notch signaling. Biochem
1032 Biophys Res Commun. 2014;453:235–42.

1033 32. Heifetz A, Keenan RW, Elbein AD. Mechanism of action of tunicamycin on the UDP-
1034 GlcNAc:dolichyl-phosphate Glc-NAc-1-phosphate transferase. Biochemistry.
1035 1979;18:2186–92.

1036 33. Elbein AD. Inhibitors of the biosynthesis and processing of N-linked oligosaccharide chains.
1037 Annu Rev Biochem. 1987;56:497–534.

1038 34. Rademacher TW, Parekh RB, Dwek RA. Glycobiology. Annual Review of Biochemistry.
1039 1988;57:785–838.

1040 35. Narasimhan S. Control of glycoprotein synthesis. UDP-GlcNAc:glycopeptide beta 4-N-
1041 acetylglucosaminyltransferase III, an enzyme in hen oviduct which adds GlcNAc in beta 1-

1042 4 linkage to the beta-linked mannose of the trimannosyl core of N-glycosyl
1043 oligosaccharides. J Biol Chem. 1982;257:10235–42.

1044 36. Gu J, Nishikawa A, Tsuruoka N, Ohno M, Yamaguchi N, Kangawa K, et al. Purification and
1045 characterization of UDP-N-acetylglucosamine: alpha-6-D-mannoside beta 1-6N-
1046 acetylglucosaminyltransferase (N-acetylglucosaminyltransferase V) from a human lung
1047 cancer cell line. J Biochem. 1993;113:614–9.

1048 37. Longmore GD, Schachter H. Product-identification and substrate-specificity studies of the
1049 GDP-L-fucose:2-acetamido-2-deoxy-beta-D-glucoside (FUC goes to Asn-linked GlcNAc)
1050 6-alpha-L-fucosyltransferase in a Golgi-rich fraction from porcine liver. Carbohydr Res.
1051 1982;100:365–92.

1052 38. Song Y, Aglipay JA, Bernstein JD, Goswami S, Stanley P. The bisecting GlcNAc on N-
1053 glycans inhibits growth factor signaling and retards mammary tumor progression. Cancer
1054 Res. 2010;70:3361–71.

1055 39. Staudacher E, Altmann F, Wilson IB, März L. Fucose in N-glycans: from plant to man.
1056 Biochim Biophys Acta. 1999;1473:216–36.

1057 40. Wilson JR, Williams D, Schachter H. The control of glycoprotein synthesis: N-
1058 acetylglucosamine linkage to a mannose residue as a signal for the attachment of L-fucose
1059 to the asparagine-linked N-acetylglucosamine residue of glycopeptide from alpha1-acid
1060 glycoprotein. Biochem Biophys Res Commun. 1976;72:909–16.

1061 41. Okazaki A, Shoji-Hosaka E, Nakamura K, Wakitani M, Uchida K, Kakita S, et al. Fucose
1062 depletion from human IgG1 oligosaccharide enhances binding enthalpy and association rate
1063 between IgG1 and FcgammaRIIIa. J Mol Biol. 2004;336:1239–49.

1064 42. Osumi D, Takahashi M, Miyoshi E, Yokoe S, Lee SH, Noda K, et al. Core fucosylation of
1065 E-cadherin enhances cell-cell adhesion in human colon carcinoma WiDr cells. Cancer Sci.
1066 2009;100:888–95.

1067 43. Pakkiriswami S, Couto A, Nagarajan U, Georgiou M. Glycosylated Notch and Cancer. Front
1068 Oncol. 2016;6:37.

1069 44. Lis H, Sharon N. Lectins: Carbohydrate-Specific Proteins That Mediate Cellular
1070 Recognition. Chem Rev. 1998;98:637–74.

1071 45. Ghazarian H, Idoni B, Oppenheimer SB. A glycobiology review: carbohydrates, lectins and
1072 implications in cancer therapeutics. Acta Histochem. 2011;113:236–47.

1073 46. Thompson R, Creavin A, O'Connell M, O'Connor B, Clarke P. Optimization of the enzyme-
1074 linked lectin assay for enhanced glycoprotein and glycoconjugate analysis. Anal Biochem.
1075 2011;413:114–22.

1076 47. Zhao L, Li G, Chan K-M, Wang Y, Tang P-F. Comparison of multipotent differentiation
1077 potentials of murine primary bone marrow stromal cells and mesenchymal stem cell line
1078 C3H10T1/2. Calcif Tissue Int. 2009;84:56–64.

1079 48. Morrow D, Scheller A, Birney YA, Sweeney C, Guha S, Cummins PM, et al. Notch-
1080 mediated CBF-1/RBP-J{kappa}-dependent regulation of human vascular smooth muscle
1081 cell phenotype in vitro. Am J Physiol Cell Physiol. 2005;289:C1188-1196.

1082 49. Chen Q, Yang F, Guo M, Wen G, Zhang C, Luong LA, et al. miRNA-34a reduces neointima
1083 formation through inhibiting smooth muscle cell proliferation and migration. J Mol Cell
1084 Cardiol. 2015;89 Pt A:75–86.

1085 50. Fan H, Meng W, Kilian C, Grams S, Reutter W. Domain-specific N-glycosylation of the
1086 membrane glycoprotein dipeptidylpeptidase IV (CD26) influences its subcellular
1087 trafficking, biological stability, enzyme activity and protein folding. Eur J Biochem.
1088 1997;246:243–51.

1089 51. Li L-B, Chen N, Ramamoorthy S, Chi L, Cui X-N, Wang LC, et al. The role of N-
1090 glycosylation in function and surface trafficking of the human dopamine transporter. J Biol
1091 Chem. 2004;279:21012–20.

1092 52. Stanley P. What Have We Learned from Glycosyltransferase Knockouts in Mice? J Mol
1093 Biol. 2016;428:3166–82.

1094 53. Boskovski MT, Yuan S, Pedersen NB, Goth CK, Makova S, Clausen H, et al. The
1095 heterotaxy gene GALNT11 glycosylates Notch to orchestrate cilia type and laterality.
1096 Nature. 2013;504:456–9.

1097 54. Matsumoto K, Ayukawa T, Ishio A, Sasamura T, Yamakawa T, Matsuno K. Dual Roles of
1098 O-Glucose Glycans Redundant with Monosaccharide O-Fucose on Notch in Notch
1099 Trafficking. J Biol Chem. 2016;291:13743–52.

1100 55. Ogawa M, Tashima Y, Sakaguchi Y, Takeuchi H, Okajima T. Contribution of extracellular
1101 O-GlcNAc to the stability of folded epidermal growth factor-like domains and Notch1
1102 trafficking. Biochem Biophys Res Commun. 2020;526:184–90.

1103 56. Allam H, Johnson BP, Zhang M, Lu Z, Cannon MJ, Abbott KL. The glycosyltransferase
1104 GnT-III activates Notch signaling and drives stem cell expansion to promote the growth and
1105 invasion of ovarian cancer. J Biol Chem. 2017;292:16351–9.

1106 57. Tang Z, Wang A, Yuan F, Yan Z, Liu B, Chu JS, et al. Differentiation of multipotent
1107 vascular stem cells contributes to vascular diseases. Nat Commun. 2012;3:875.

1108 58. Morrow D, Guha S, Sweeney C, Birney Y, Walshe T, O'Brien C, et al. Notch and vascular
1109 smooth muscle cell phenotype. Circulation Research. 2008;103:1370–82.

1110 59. Noseda M, Fu Y, Niessen K, Wong F, Chang L, McLean G, et al. Smooth Muscle alpha-
1111 actin is a direct target of Notch/CSL. Circ Res. 2006;98:1468–70.

1112 60. Doi H, Iso T, Yamazaki M, Akiyama H, Kanai H, Sato H, et al. HERP1 inhibits myocardin-
1113 induced vascular smooth muscle cell differentiation by interfering with SRF binding to
1114 CArG box. Arterioscler Thromb Vasc Biol. 2005;25:2328–34.

1115 61. Maier MM, Gessler M. Comparative analysis of the human and mouse Hey1 promoter: Hey
1116 genes are new Notch target genes. Biochem Biophys Res Commun. 2000;275:652–60.

1117 62. Chang P-J, Boonsiri J, Wang S-S, Chen L-Y, Miller G. Binding of RBP-Jkappa (CSL)
1118 protein to the promoter of the Kaposi's sarcoma-associated herpesvirus ORF47 (gL) gene is
1119 a critical but not sufficient determinant of transactivation by ORF50 protein. Virology.
1120 2010;398:38–48.

1121 63. Tang Y, Urs S, Boucher J, Bernaiche T, Venkatesh D, Spicer DB, et al. Notch and
1122 transforming growth factor-beta (TGFbeta) signaling pathways cooperatively regulate
1123 vascular smooth muscle cell differentiation. J Biol Chem. 2010;285:17556–63.

1124 64. Hasan SS, Fischer A. Notch Signaling in the Vasculature: Angiogenesis and Angiocrine
1125 Functions. Cold Spring Harb Perspect Med. 2023;13:a041166.

1126 65. Peterson SM, Turner JE, Harrington A, Davis-Knowlton J, Lindner V, Gridley T, et al.
1127 Notch2 and Proteomic Signatures in Mouse Neointimal Lesion Formation. Arterioscler
1128 Thromb Vasc Biol. 2018;38:1576–93.

1129 66. Allam H, Aoki K, Benigno BB, McDonald JF, Mackintosh SG, Tiemeyer M, et al. Glycomic
1130 analysis of membrane glycoproteins with bisecting glycosylation from ovarian cancer
1131 tissues reveals novel structures and functions. J Proteome Res. 2015;14:434–46.

1132 77. Maupin KA, Liden D, Haab BB. The fine specificity of mannose-binding and galactose-
1133 binding lectins revealed using outlier motif analysis of glycan array data. Glycobiology.
1134 2012;22:160–9.

1135 68. Nagae M, Soga K, Morita-Matsumoto K, Hanashima S, Ikeda A, Yamamoto K, et al.
1136 Phytohemagglutinin from Phaseolus vulgaris (PHA-E) displays a novel glycan recognition
1137 mode using a common legume lectin fold. Glycobiology. 2014;24:368–78.

1138 69. Yu G, Nishimura M, Arawaka S, Levitan D, Zhang L, Tandon A, et al. Nicastrin modulates
1139 presenilin-mediated notch/glp-1 signal transduction and betaAPP processing. Nature.
1140 2000;407:48–54.

1141 70. Yagi H, Saito T, Yanagisawa M, Yu RK, Kato K. Lewis X-carrying N-glycans regulate the
1142 proliferation of mouse embryonic neural stem cells via the Notch signaling pathway. J Biol
1143 Chem. 2012;287:24356–64.

1144 71. Kakuda S, Haltiwanger RS. Deciphering the Fringe-Mediated Notch Code: Identification of
1145 Activating and Inhibiting Sites Allowing Discrimination between Ligands. Dev Cell.
1146 2017;40:193–201.

1147 72. Stahl M, Uemura K, Ge C, Shi S, Tashima Y, Stanley P. Roles of Pofut1 and O-fucose in
1148 mammalian Notch signaling. J Biol Chem. 2008;283:13638–51.

1149 73. Sun X, Tie HC, Chen B, Lu L. Glycans function as a Golgi export signal to promote the
1150 constitutive exocytic trafficking. J Biol Chem. 2020;295:14750–62.

1151 74. Skrenkova K, Lee S, Lichnerova K, Kaniakova M, Hansikova H, Zapotocky M, et al. N-
1152 Glycosylation Regulates the Trafficking and Surface Mobility of GluN3A-Containing
1153 NMDA Receptors. Front Mol Neurosci. 2018;11:188.

1154 75. Janezic EM, Lauer SM-L, Williams RG, Chungyoun M, Lee K-S, Navaluna E, et al. N-
1155 glycosylation of α1D-adrenergic receptor N-terminal domain is required for correct
1156 trafficking, function, and biogenesis. Sci Rep. 2020;10:7209.

1157 76. Weis WI, Drickamer K. Structural basis of lectin-carbohydrate recognition. Annu Rev
1158 Biochem. 1996;65:441–73.

1159 77. Zhao Y, Sato Y, Isaji T, Fukuda T, Matsumoto A, Miyoshi E, et al. Branched N-glycans
1160 regulate the biological functions of integrins and cadherins. FEBS J. 2008;275:1939–48.

1161 78. Yamamoto K, Ito S, Yasukawa F, Konami Y, Matsumoto N. Measurement of the
1162 carbohydrate-binding specificity of lectins by a multiplexed bead-based flow cytometric
1163 assay. Anal Biochem. 2005;336:28–38.

1164 79. Lee TK, Koh AS, Cui Z, Pierce RH, Ballatori N. N-glycosylation controls functional activity
1165 of Oatp1, an organic anion transporter. Am J Physiol Gastrointest Liver Physiol.
1166 2003;285:G371-381.

80. Ding Y, Uchida K, Aizawa S-I, Murphy K, Berezuk A, Khursigara CM, et al. Effects of N-glycosylation site removal in archaellins on the assembly and function of archaella in Methanococcus maripaludis. PLoS One. 2015;10:e0116402.

81. West MB, Wickham S, Quinalty LM, Pavlovicz RE, Li C, Hanigan MH. Autocatalytic cleavage of human gamma-glutamyl transpeptidase is highly dependent on N-glycosylation at asparagine 95. J Biol Chem. 2011;286:28876–88.

82. Hsiao C-C, Cheng K-F, Chen H-Y, Chou Y-H, Stacey M, Chang G-W, et al. Site-specific N-glycosylation regulates the GPS auto-proteolysis of CD97. FEBS Lett. 2009;583:3285–90.

83. Branza-Nichita N, Negroiu G, Petrescu AJ, Garman EF, Platt FM, Wormald MR, et al. Mutations at critical N-glycosylation sites reduce tyrosinase activity by altering folding and quality control. J Biol Chem. 2000;275:8169–75.

84. Brack AS, Conboy IM, Conboy MJ, Shen J, Rando TA. A temporal switch from notch to Wnt signaling in muscle stem cells is necessary for normal adult myogenesis. Cell Stem Cell. 2008;2:50–9.

85. Acosta H, López SL, Revinski DR, Carrasco AE. Notch destabilises maternal beta-catenin and restricts dorsal-anterior development in Xenopus. Development. 2011;138:2567–79.

86. Tanaka S, Terada K, Nohno T. Canonical Wnt signaling is involved in switching from cell proliferation to myogenic differentiation of mouse myoblast cells. J Mol Signal. 2011;6:12.

87. Hayward P, Brennan K, Sanders P, Balayo T, DasGupta R, Perrimon N, et al. Notch modulates Wnt signalling by associating with Armadillo/beta-catenin and regulating its transcriptional activity. Development. 2005;132:1819–30.

88. Itakura Y, Nakamura-Tsuruta S, Kominami J, Sharon N, Kasai K-I, Hirabayashi J. Systematic comparison of oligosaccharide specificity of Ricinus communis agglutinin I and Erythrina lectins: a search by frontal affinity chromatography. J Biochem. 2007;142:459–69.

89. Delorme E, Lorenzini T, Giffin J, Martin F, Jacobsen F, Boone T, et al. Role of glycosylation on the secretion and biological activity of erythropoietin. Biochemistry. 1992;31:9871–6.

90. Ishikawa H, Uchida T, Takahashi S, Ishimori K, Morishima I. Ligand migration in human myoglobin: steric effects of isoleucine 107(G8) on O(2) and CO binding. Biophys J. 2001;80:1507–17.

91. van Berkel PH, van Veen HA, Geerts ME, de Boer HA, Nuijens JH. Heterogeneity in utilization of N-glycosylation sites Asn624 and Asn138 in human lactoferrin: a study with glycosylation-site mutants. Biochem J. 1996;319 (Pt 1) Pt 1:117–22.

92. Flack MR, Froehlich J, Bennet AP, Anasti J, Nisula BC. Site-directed mutagenesis defines the individual roles of the glycosylation sites on follicle-stimulating hormone. J Biol Chem. 1994;269:14015–20.

93. Jacob GS. Glycosylation inhibitors in biology and medicine. Curr Opin Struct Biol. 1995;5:605–11.

Acknowledgments

Funding:

Irish Research Council (IRC) GOIPG/2016/1529 (EC)
Irish Research Council (IRC) GOIPG/2014/43 (MDL)
Government of Saudi Arabia ID: IR15208 (JG)
National Institutes of Health R01-AA024082 (EMR)
Science Foundation Ireland (SFI) award 11-PI-1128 (PAC)
Health Research Board (HRB), Ireland HRA-POR-2015-1315 (PAC)

Author contributions

Conceptualization: PAC, EC
Methodology: EC, AO, BOC, YG, RH, MDL
Investigation: EC, AO,
Visualization: SFB
Supervision: PAC
Writing—original draft: EC, AO
Writing—review & editing: AO, EMR, PAC

Competing interests: Authors declare that they have no competing interests.

Data and materials availability: The datasets used and/or analysed during the current study are available from the corresponding author on reasonable request. All data are available in the main text or the supplementary materials.

Figures and Tables

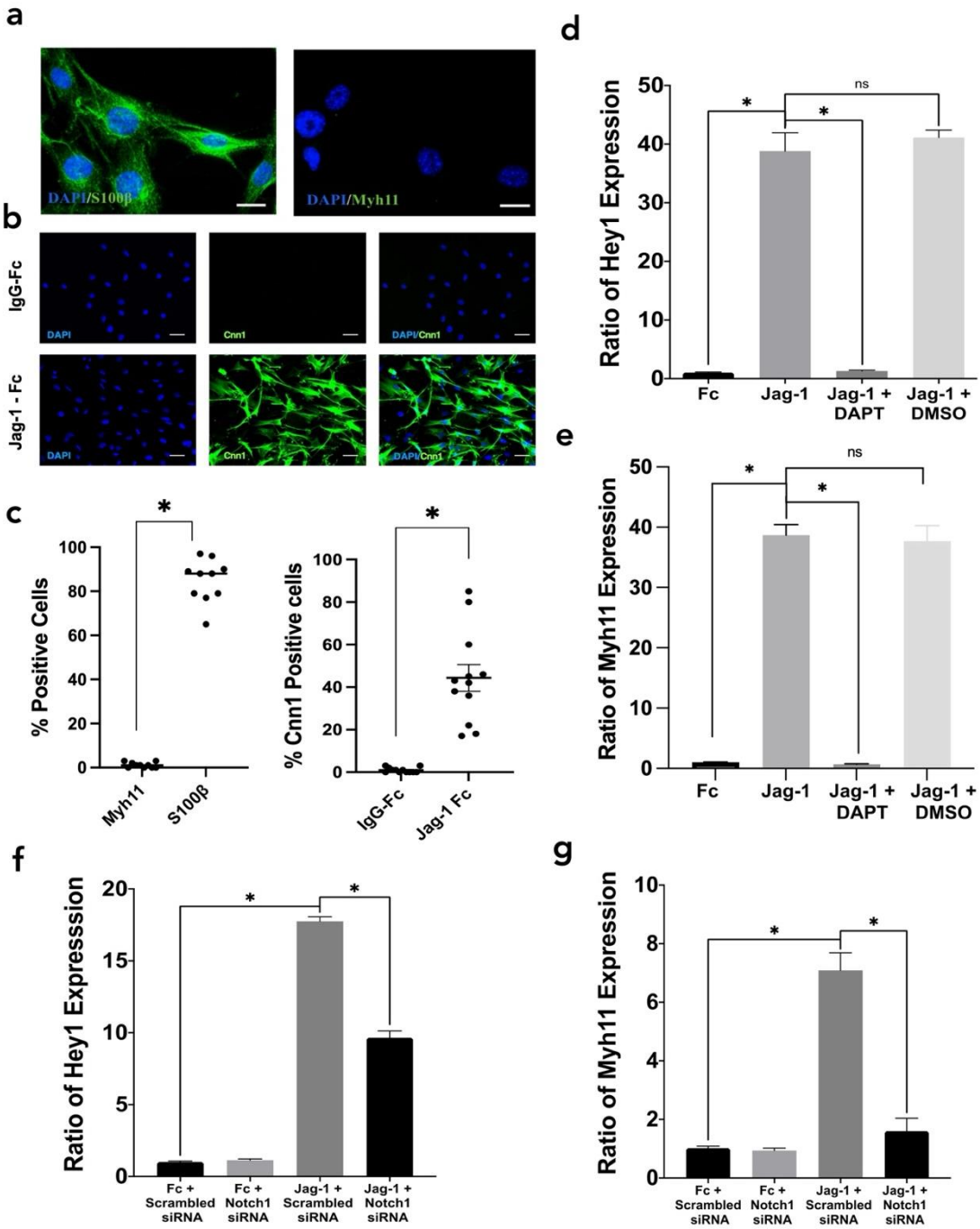

Figure 1: Jagged-1 activation of Notch1 signalling and SMC differentiation in S100β mVSCs. Immunocytochemical analysis of (a) Myh11 and S100β protein expression in untreated mVSCs and (b) Cnn1 expression in aortic S100β mVSCs treated with recombinant immobilised Jagged-1 (Jag-1 Fc) or IgG-Fc at 1μg/mL in MM1 media after 7 days. Scale bar = 25μm. (c) Mean percentage of Myh11, S100β and Cnn1 positive cells. DAPI was used to stain nuclei. Positive cells were counted and compared against total DAPI cell count. Data are the mean ± SEM and representative of n=3 *$p \leq 0.05$. (d-g) Real-time qRT-PCR analysis of *Hey1* and *Myh11* mRNA levels in S100β mVSCs treated with recombinant immobilised Jagged-1 (Jag-1 Fc) or IgG-Fc (Fc) at 1μg/mL for 48 hrs with or without prior treatment of cells with a γ-secretase inhibitor, DAPT versus DMSO control (d, e) and following Notch1 receptor knockdown (f-g) versus scrambled control. The gene, hypoxanthine phosphoribosyltransferase *(hprt*) was used as a housekeeping control. Data are the mean ± SEM and representative of n=3 *$p \leq 0.05$

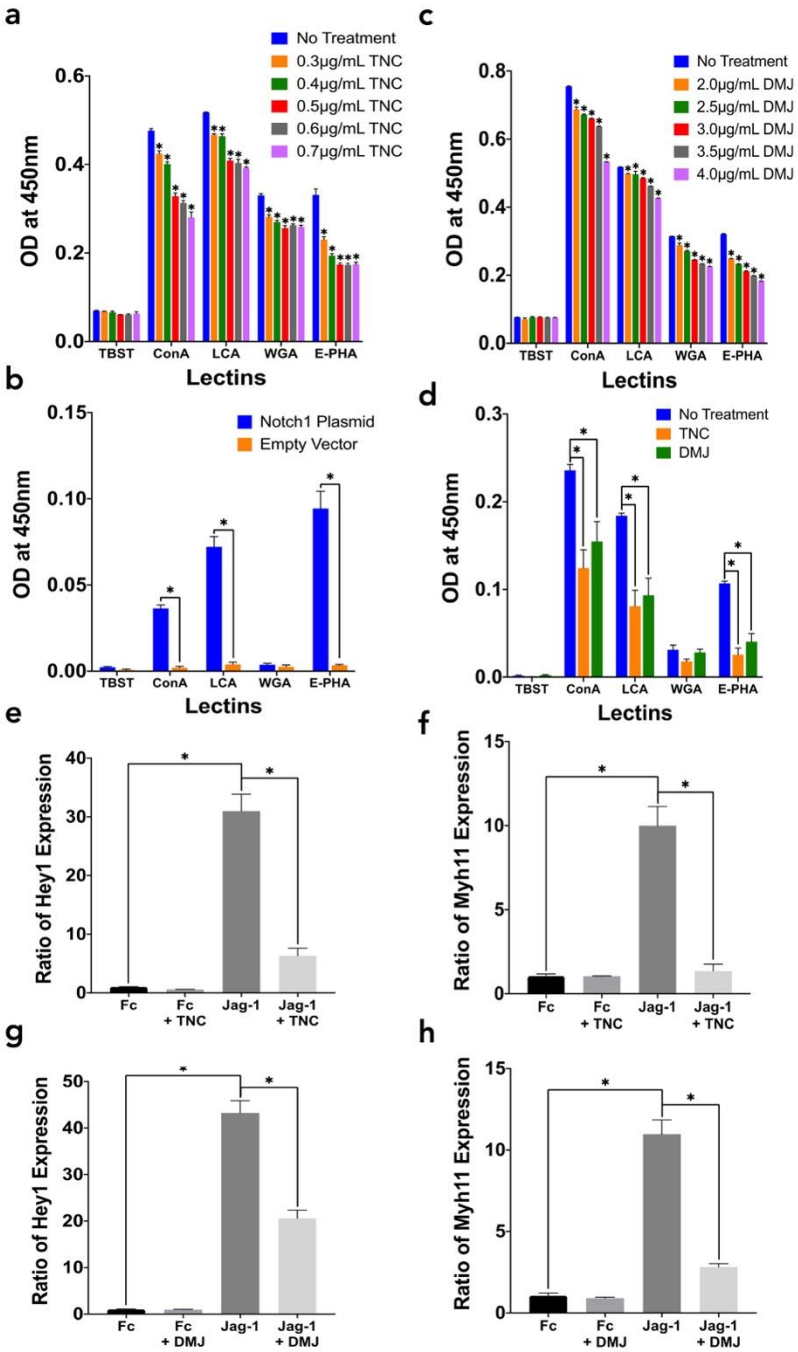

Figure 2: Chemical inhibition of N-glycosylation (TNC and DMJ) on lectin binding and Jagged-1 activation of Notch1 signalling and SMC differentiation in S100β mVSCs. ELLA analysis of N-glycan specific lectin binding of whole cell lysates (a, c) and immunoprecipitated ectopic expression of the Notch1 receptor (b, d) following treatment of S100β mVSC with a range of TNC (a, b) and DMJ (c, d) concentrations for 48 h at 37ºC. Data are presented as the mean absorbance value at 450 nm normalised to the negative control TBST sample. Data are the mean ± SEM and representative of n=3 *$p \leq 0.05$ compared to the non-treated sample probed with the same lectins. Real-time qRT-PCR analysis of *Hey1* and *Myh11* mRNA levels in S100β mVSCs treated with recombinant immobilised Jagged-1 (Jag-1 Fc) or IgG-Fc (Fc) at 1μg/mL in MM1 media after 48 hrs following ectopic expression of the Notch1 receptor with or without prior treatment of cells with TNC (0.5μg/mL) (e, f) and DMJ (4μg/mL) (g-h). The gene, hypoxanthine phosphoribosyltransferase *(hprt*) was used as a housekeeping control. Data are the mean ± SEM and representative of n=3 *$p \leq 0.05$

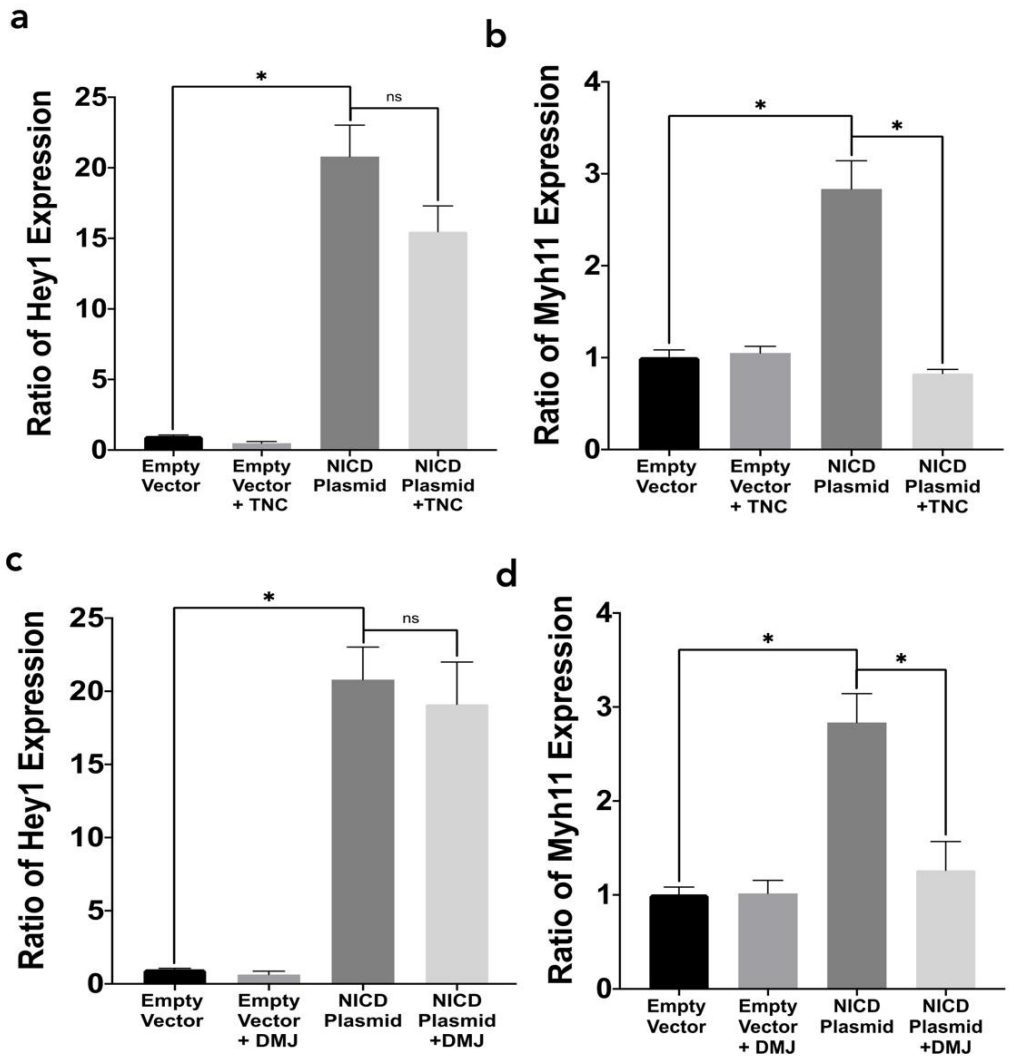

Figure 3: **Chemical inhibition of N-glycosylation (TNC and DMJ) on Notch1 intracellular domain (NICD) activation of Notch signalling and SMC differentiation in S100β mVSCs**. Real-time qRT-PCR analysis of *Hey1* (a, c) and *Myh11* (b, d) mRNA levels in S100β mVSCs following ectopic expression of the Notch1 NICD after 48 hrs with or without prior treatment of cells with TNC (0.5µg/mL) (a, b) or DMJ (4µg/mL) (c-d). The gene, hypoxanthine phosphoribosyltransferase *(hpr*t) was used as a housekeeping control. Data are the mean ± SEM and representative of n=3 *$p \leq 0.05$.

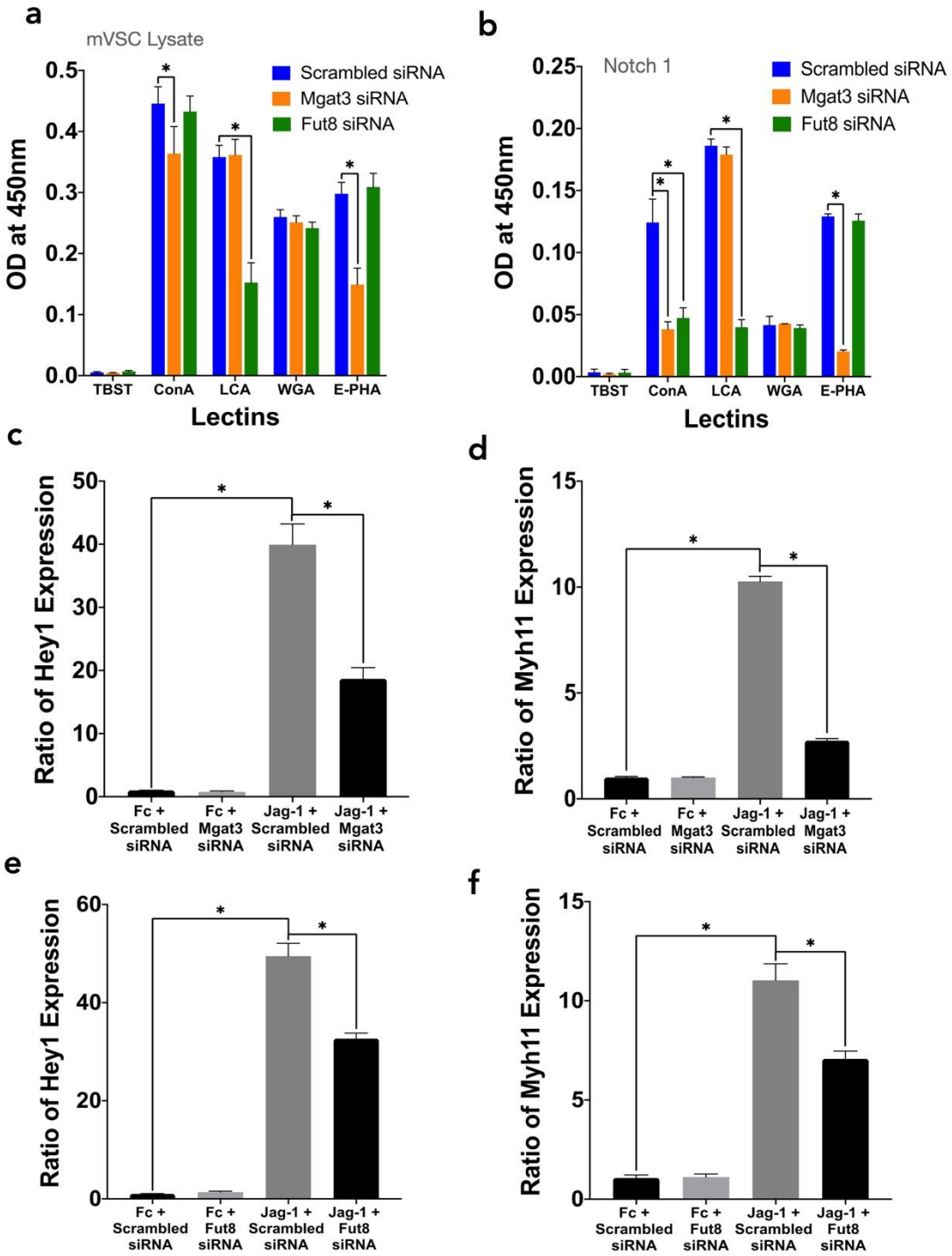

Figure 4: *Mgat3* and *Fut8* knockdown on lectin binding, Notch signalling, and SMC differentiation in S100β mVSCs. ELLA analysis of N-glycan specific lectin binding of whole cell lysate (a) and immunoprecipitated ectopic expression of the Notch1 receptor (b) following *Mgat3* and *Fut8* knockdown with specific siRNA duplexes (25nM) versus scrambled control. Data are presented as the mean absorbance value at 450 nm normalised to the negative control TBST sample. Data are the mean ± SEM and representative of n=3 *$p \leq 0.05$. compared to the non-treated sample probed with the same lectins. Real-time qRT-PCR analysis of *Hey1* (c, e) and *Myh11* (d, f) mRNA levels in S100β mVSCs treated with recombinant immobilised Jagged-1 (Jag-1 Fc) or IgG-Fc (Fc) at 1µg/mL after 48 hrs following *Mgat3* (c, d) or *Fut8* (e, f) knockdown with specific siRNA duplexes (25nM) versus scrambled control. The gene, hypoxanthine phosphoribosyltransferase *(hpr*t) was used as a housekeeping control. Data are the mean ± SEM and representative of n=3 *$p \leq 0.05$

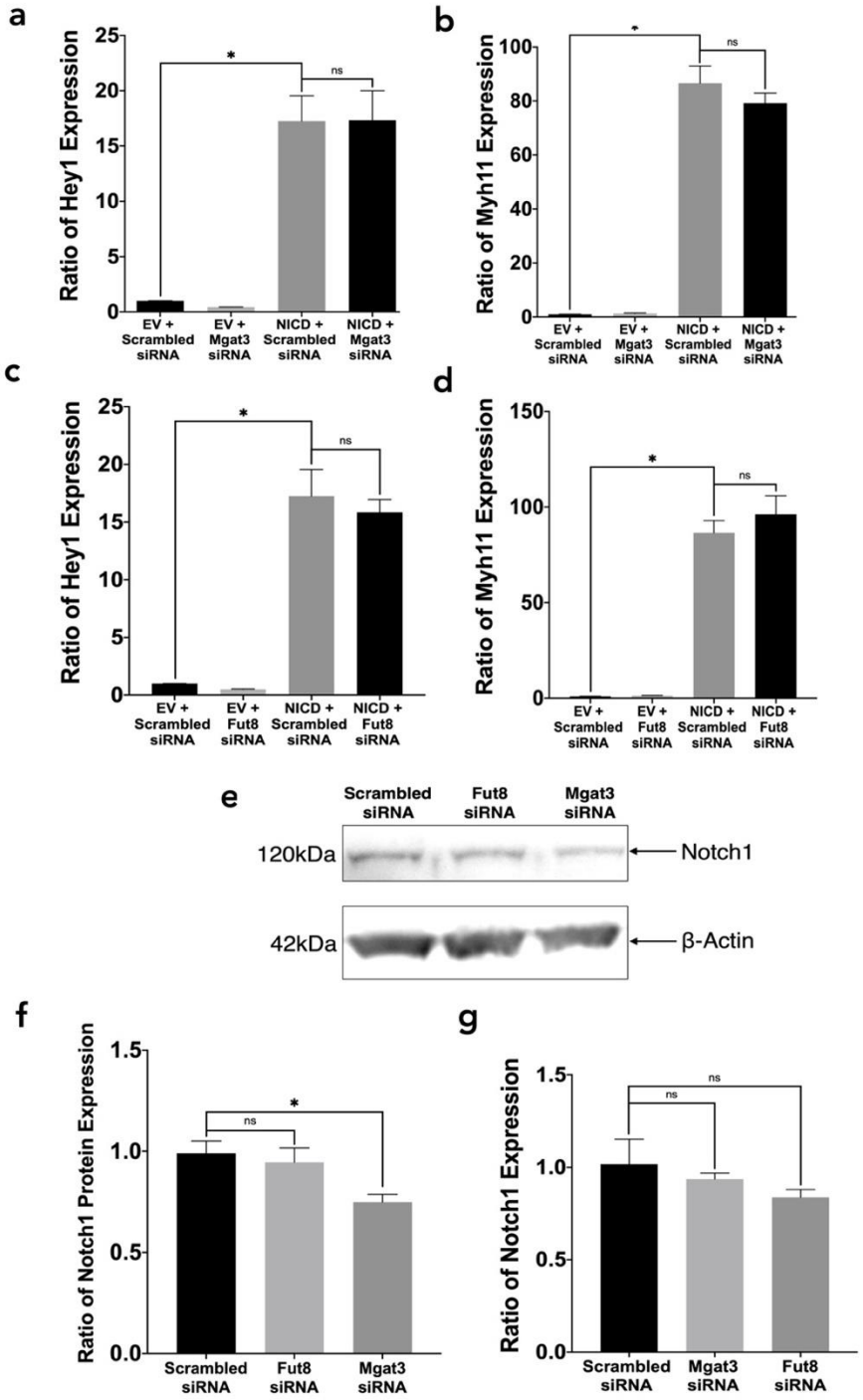

Figure 5: *Mgat3* and *Fut8* knockdown on Notch1 intracellular domain (NICD) activation of Notch signalling and SMC differentiation in S100β mVSCs. Real-time qRT-PCR analysis of *Hey1* (a, c) and *Myh11* (b, d) mRNA levels in S100β mVSCs stimulated by ectopic expression of Notch1 NICD after 48 hrs following *Mgat3* (a, b) and *Fut8* (c, d) knockdown with specific siRNA duplexes (25nM) versus scrambled control. The gene, hypoxanthine phosphoribosyltransferase *(hprt*) was used as a housekeeping control. Immunoblot analysis of Notch1 protein levels (e, f) and real-time qRT-PCR analysis of *Notch1* mRNA levels (g) following *Mgat3* or *Fut8* knockdown with specific siRNA duplexes (25nM) versus scrambled control. (e) a representative immunoblot image of Notch1 bands at 120kDa and β-actin bands at 42kDa. (f) Densitometry analysis of the intensity of Notch1 bands normalised to the β-actin loading control. Notch1 protein levels given as ratio of expression relative to the untreated negative control sample. (g) *Notch1* mRNA levels. Data are the mean ± SEM and representative of n=3, ns or *$p \leq 0.05$.

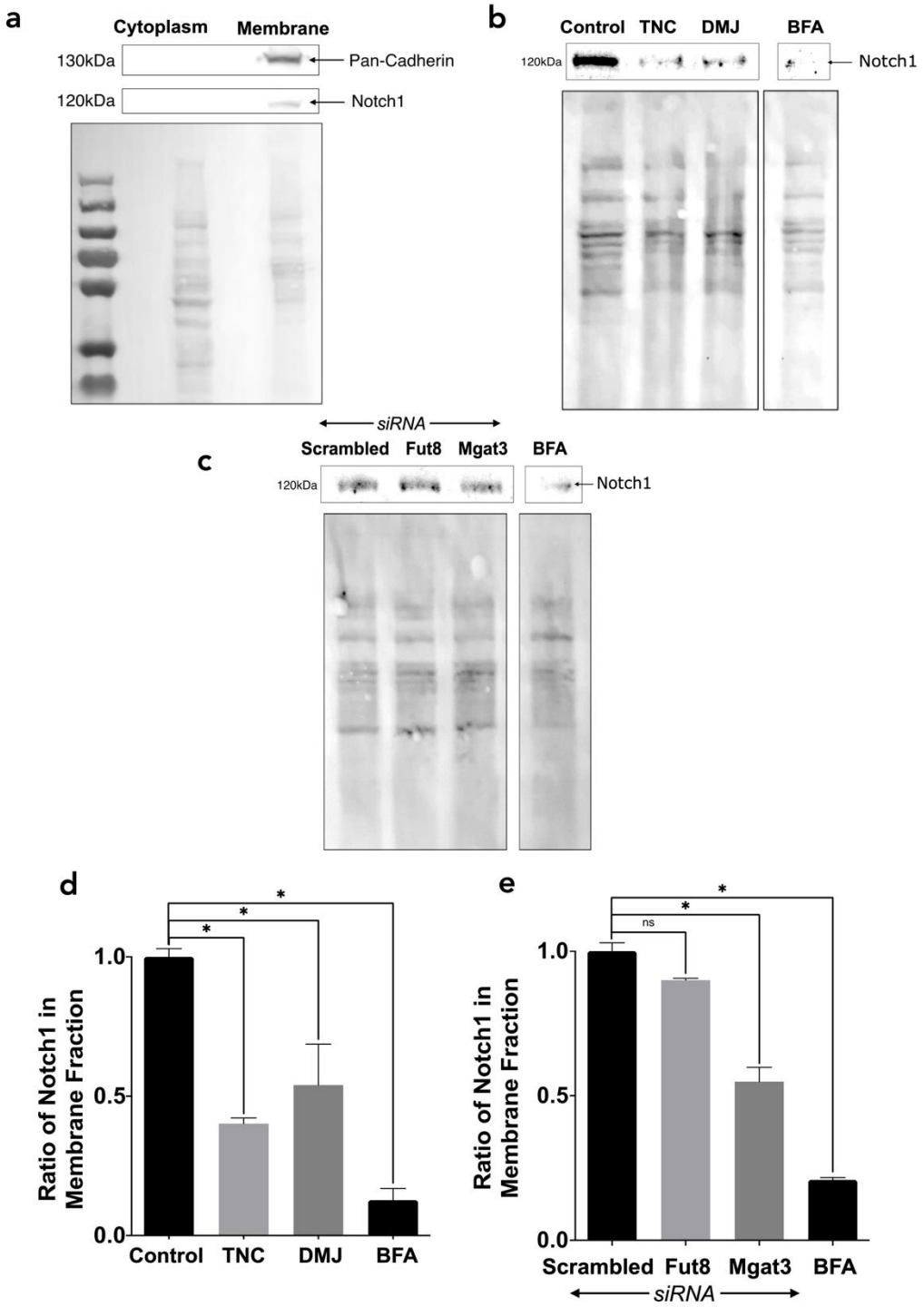

Figure 6: Chemical inhibition of N-glycosylation (TNC and DMJ) and *Mgat3* and *Fut8* knockdown on membrane localisation of the Notch1 receptor. (a) Membrane fractionation was carried out on S100β mVSCs lysates before Notch1 and Pan-Cadherin protein expression was assessed in cytoplasmic and membrane fractions, respectively. A representative immunoblot image of Notch1 at 120kDa (upper panel) and Ponceau S staining (lower panel) in each fraction. (b) Notch 1 protein expression in the membrane fractions of whole lysates from S100β mVSCs treated with TNC (0.5μg/mL), DMJ (4μg/mL) or 1 X BFA for 48 h at 37ºC. (c) Notch 1 protein expression in the membrane fraction of whole lysates from S100β mVSCs following *Mgat3* or *Fut8* knockdown compared to scrambled control or cells treated with 1 X BFA. (d, e) Densitometry analysis of the intensity of Notch1 bands normalised to the Ponceau S loading control. Notch1 protein levels in membrane fraction presented as the ratio of expression relative to the untreated negative control or scrambled control. Data are the mean ± SEM and representative of n=3, ns or *$p \leq 0.05$

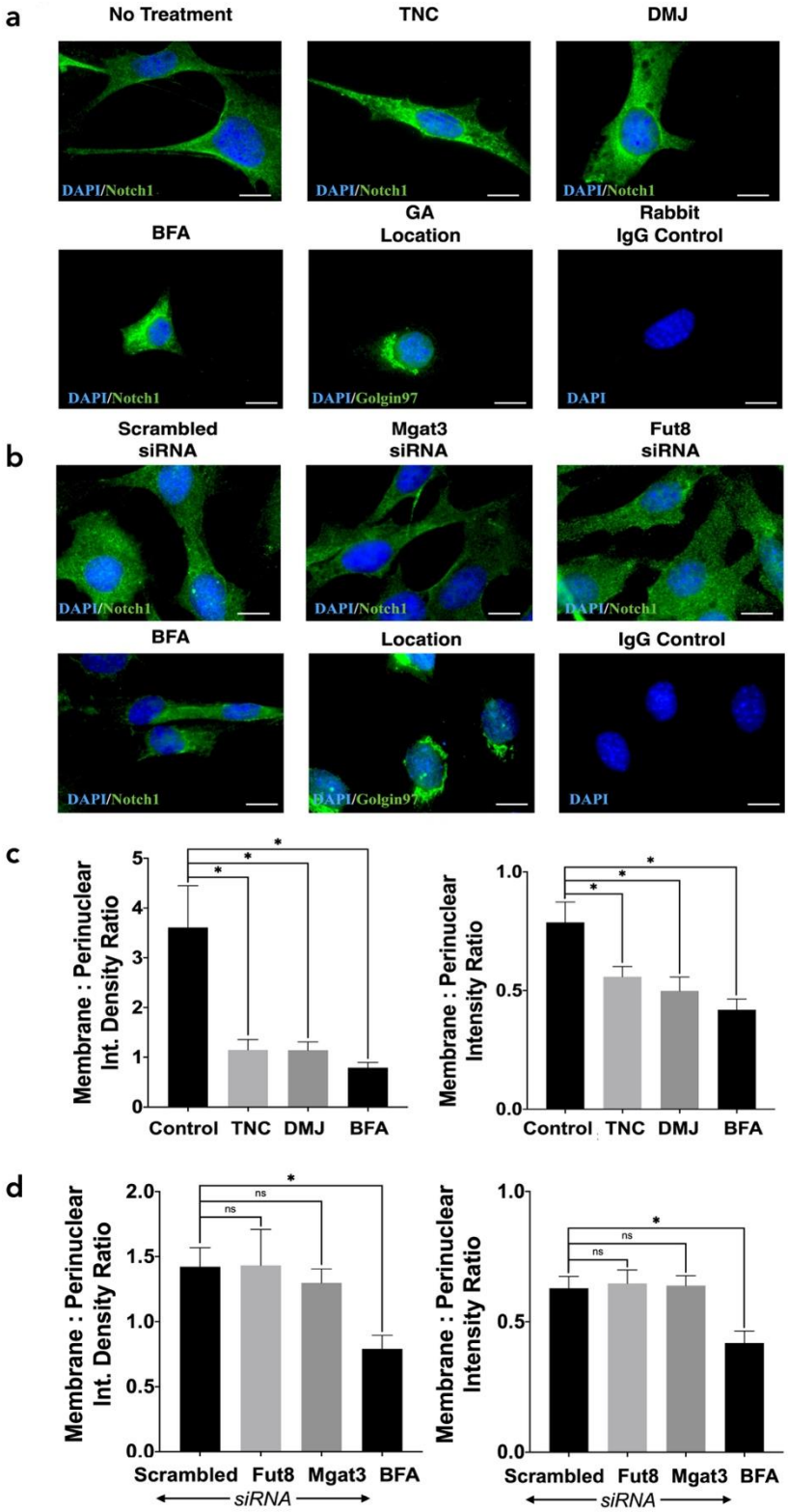

Figure 7: Chemical inhibition of N-glycosylation (TNC and DMJ) and *Mgat3* and *Fut8* knockdown on Notch1 receptor trafficking. Localization of Notch 1 receptor expression in S100β mVSCs treated with (a) TNC (0.5µg/mL), DMJ (4µg/mL) or 1 X BFA or (b) following *Mgat3* or *Fut8* knockdown, compared to untreated negative control sample, scrambled control, or treated with 1 X BFA for 48 h at 37ºC. Representative images at 60X magnification. Location of the GA was confirmed using Golgin-97. Scale bar = 10µm. (c-d) ImageJ used to calculate the ratio of Membrane: Perinuclear fluorescence using (c) integrated density and (d) mean fluorescence intensity values. Data are the mean ± SEM and representative of n=3, ns or *$p \leq 0.05$.

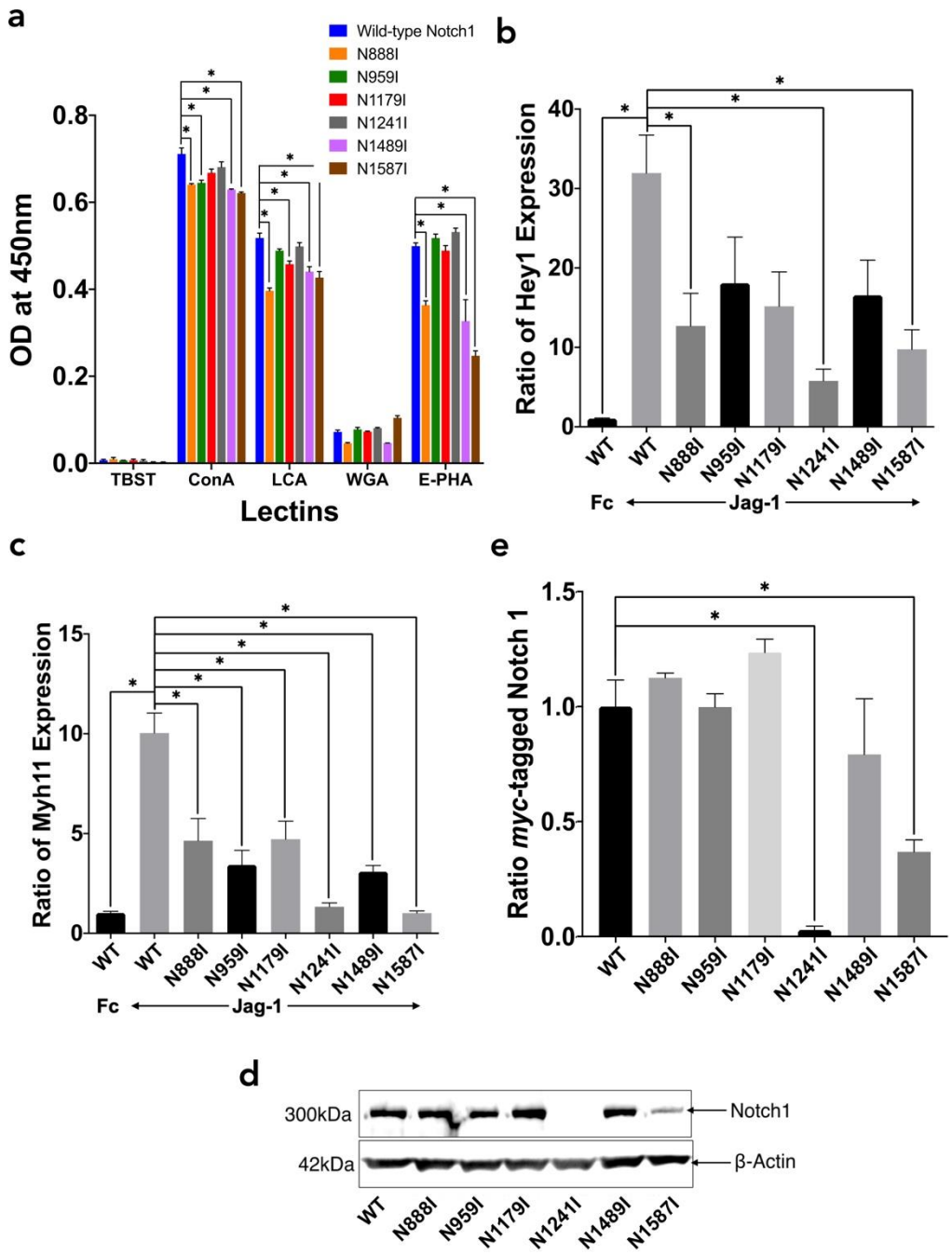

Figure 8: Site-directed mutagenesis of asparagine residues on the Notch1 ECD receptor on lectin binding, Notch signalling, and SMC differentiation in C3H10T1/2 cells. (a) ELLA analysis of N-glycan specific lectin binding of immunoprecipitated wild-type and mutant Notch1 receptors (N888I, N959I, N1179I, N1241I, N1489I and N1587I) from puromycin selected C3H10T1/2 cells. Data are presented as the mean absorbance value at 450nm normalised to the negative control TBST sample and the IgG immunoprecipitation control. (b, c) Real-time qRT-PCR analysis of Jag-1 stimulated *Hey1* (b) and *Myh11* (c) mRNA levels in C3H10T1/2 cells following ectopic expression of wild-type and mutant Notch1 receptors. Cells were treated with recombinant immobilised Jagged-1 (Jag-1 Fc) or IgG-Fc (Fc) at 1µg/mL in MM1 media after 48 hrs. The gene, hypoxanthine phosphoribosyltransferase *(hpr*t) was used as a housekeeping control. (d) Immunoprecipitated wildtype (WT) and mutant Notch1 receptor expression. A representative immunoblot image of full-length Notch1 bands at 300kDa and β-actin bands at 42kDa. (e) Densitometry analysis of the intensity of Notch1 bands normalised to the β-actin loading control. Full-length Notch1 protein levels presented as the ratio of expression relative to the wild-type Notch1 control. Data are the mean ± SEM and representative of n=3, ns or *$p \leq 0.05$.

Lectin	Binding specificity
ConA	Internal α-linked mannose
LCA	Internal α-linked mannose. Strongest affinity for mannose core with α-1,6 linked fucose bound to primary GlcNAc residue
WGA	High affinity for terminal GlcNAc and dimers/trimers of GlcNAc. Also reacts with chitobiose core of N-linked glycans, specifically the Man β(1,4)GlcNAc β(1,4)GlcNAc trisaccharide. Can also bind GlcNAc in O-glycans
E-PHA	Binds complex N-glycans. Usually at branching point from mannose core, specifically Galβ4GlcNAcβ2Manα6; (GlcNAcβ4); (GlcNAcβ4Manα3). Strong affinity for complex bisecting N-glycan structure.

Table I: The binding specificities of lectins. The binding specificity of Concanavalin A (ConA), Lens Culinaris Agglutinin (LCA), Wheat germ agglutinin (WGA) and Phaseolus vulgaris lectin E (E-PHA) on the ELLA assay.

Asn Site	N-Glycan Structures	Possible Role of Glycan
N888	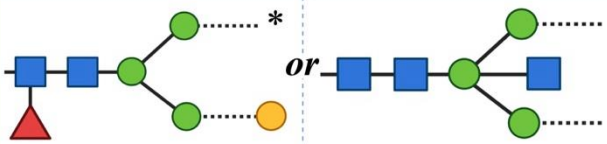	Regulation of receptor folding/cleavage
N959	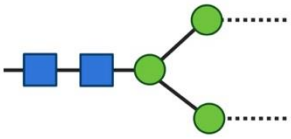	Impacts non-canonical Notch signalling
N1179	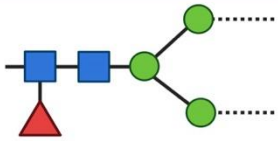	Impacts non-canonical Notch signalling
N1241	No N-glycan present 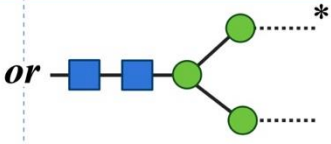	Regulation of receptor degradation
N1489	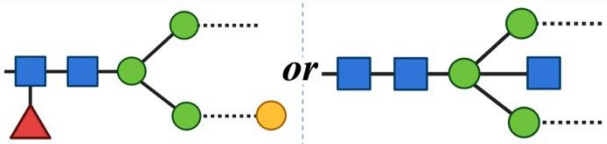	Impacts non-canonical Notch signalling
N1587	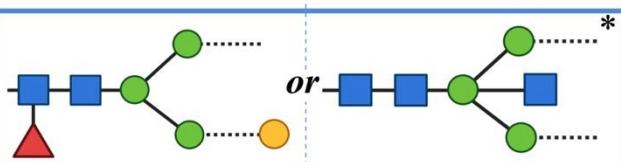	Regulation of receptor degradation

* Indicates most likely structure based on Notch1 expression and signalling data

Table II: N-Glycan Structures and Possible Roles on the Notch1 Receptor. The N-glycan structures and possible role of each glycan in regulating Notch signalling at specific asparagine residues on the Notch 1 ECD.